HHS Public Access

Author manuscript

J Control Release. Author manuscript; available in PMC 2020 June 28.

Published in final edited form as:

J Control Release. 2019 June 28; 304: 216–232. doi:10.1016/j.jconrel.2019.04.041.

Subchronic Toxicity of Silica Nanoparticles as a Function of Size and Porosity

Raziye Mohammadpour[1], **Mostafa Yazdimamaghani**[1,2,#], **Darwin L. Cheney**[1], **Jolanta Jedrzkiewicz**[3], **Hamidreza Ghandehari**[1,2,4,*]

[1]Utah Center for Nanomedicine, Nano Institute of Utah, University of Utah, Salt Lake City, Utah, United States

[2]Department of Pharmaceutics and Pharmaceutical Chemistry, University of Utah, Salt Lake City, Utah, United States

[3]Department of Pathology, University of Utah, Salt Lake City, Utah, United States

[4]Department of Bioengineering, University of Utah, Salt Lake City, Utah, United States

Abstract

Despite increasing reports of using silica nanoparticles (SNPs) for controlled drug delivery applications, their long-term toxicity profile following intravenous administration remains unexplored. Herein, we investigated the acute (10-day) and subchronic (60-day and 180-day) toxicity of nonporous SNPs of approximately 50 nm (Stöber SNPs50) and approximately 500 nm in diameter (Stöber SNPs500), and mesoporous SNPs of approximately 500 nm in diameter (MSNPs500) upon single-dose intravenous injection into male and female immune-competent inbred BALB/C mice. The Maximum Tolerated Dose (MTD) of the particles was determined 10 days post-injection. The MTD of SNPs was administered and toxicity evaluated over 60 and 180 days. Results demonstrate that Stöber SNPs50 exhibit systemic toxicity with MTD of 103 ± 11 $mg.kg^{-1}$ for female and 100 ± 6 $mg.kg^{-1}$ for male mice, respectively. Toxicity was alleviated by increasing the size of the particles (Stöber SNPs500). MTD values of 303 ± 4 $mg.kg^{-1}$ for female and 300 ± 13 $mg.kg^{-1}$ for male were observed for Stöber SNPs500. Mesoporous SNPs500 showed considerable systemic sex-related toxicity, with MTDs ranging from 40 ± 2 $mg.kg^{-1}$ to 95 ± 2 $mg.kg^{-1}$ for male and female mice, respectively. Studies of SNPs showed blood toxicity as a function of physiochemical properties such as significant differences in the mean corpuscular hemoglobin (MCHC) and platelet number at day 10 and white blood cell count at day 60. Histological examination also showed size-, porosity- and time-dependent tissue toxicity. Stöber

*Corresponding author at: 36 S. Wasatch Dr. Salt Lake City, Utah, USA, 84112, hamid.ghandehari@utah.edu, Ph: 801-587-1566, Fax: 801-581-6321.

#Present address: Pharmacoengineering and Molecular Pharmaceutics, Center for Nanotechnology in Drug Delivery, UNC Eshelman School of Pharmacy, Lineberger Comprehensive Cancer Center, UNC School of Medicine, The University of North Carolina at Chapel Hill.

Disclosure: The authors declare no commercial affiliations that might pose a potential, perceived or real conflict of interest with these studies.

SNPs500 caused major toxic effects such as lung thrombosis, cardiac wall fibrosis and calcifications, brain infarctions with necrotizing inflammatory response, infiltrate, retinal injuries with calcification and focal gliosis, renal parenchymal damage and liver lobular inflammation dependent on the dose and time of exposure. However, tissue toxicity and accumulation of SNPs in liver observed at day 10 was greater than at day 60 and much greater than at day 180. In contrast, a dramatic increase in cytokine levels was observed at day 60. Despite the relatively high doses, SNPs did not cause subchronic toxicity at day 180 after single-dose intravenous injection. However, they showed distinct differences in the 60 day *in vivo* subchronic toxicity and inflammation profile as a function of surface area and size.

Graphical abstract:

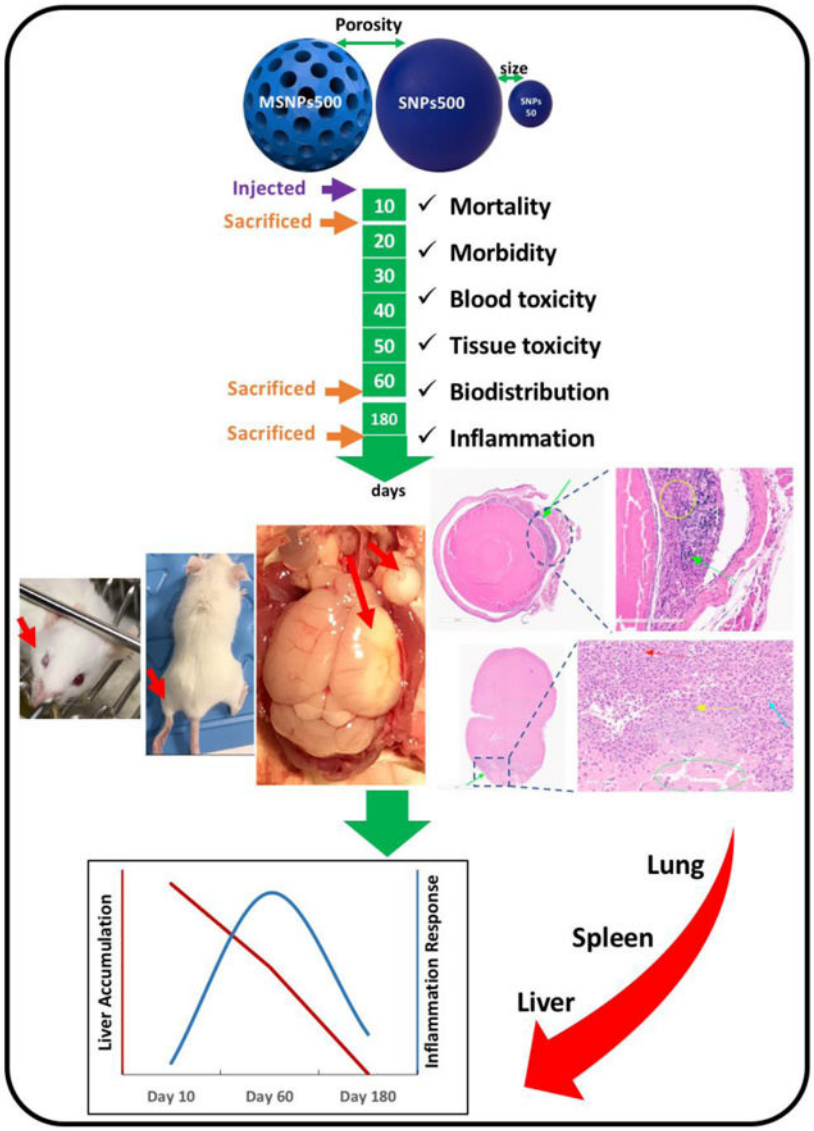

Keywords

Subchronic Toxicity; Silica Nanoparticles; Physiochemical Properties; Inflammation; Drug Delivery

Introduction:

A growing body of literature points to the potential of silica nanoparticles (SNPs) for controlled delivery applications.[1-8] A major challenge with systemic administration of inorganic nanoparticles, including SNPs are recognition by macrophages, subsequent immune response, and accumulation in the reticuloendothelial system. Accumulation of SNPs and the immune response can raise concerns about the safety of these particles depending on duration of exposure and physiochemical properties. A detailed investigation of the toxicity and inflammatory response of SNPs is needed to ensure their safe and effective use in controlled delivery applications.[9]

Toxicity assessments are classified into acute, sub-acute, subchronic, and chronic.[10] Acute toxicity studies are generally conducted over a few days and sub-acute studies typically over 4-5 weeks. A typical observation period for subchronic studies is 13 weeks and for chronic studies 18-30 months.[11] The United States Department of Health and Human Services National Toxicology Program categorizes toxicology studies into short term (14 days and 13 weeks) and long-term (2 years).[10] Studies from our laboratory [12-15] and others [16-18] have focused on evaluating the short-term toxicity of SNPs following intravenous administration. However, little information is available regarding the long-term safety of SNPs following intravenous injection.

It is clear that the physicochemical attributes of SNPs can play an important role in causing adverse effects *in vitro* and *in vivo*.[12, 13, 15, 19-22] For example, our *in vitro* assessments have shown that mesoporous SNPs are less toxic on macrophage cells (Raw 264.7) compared to similar sized Stöber nanoparticles, whereas *in vivo* the Maximum Tolerated Dose (MTD) of unmodified mesoporous SNPs is lower than the MTD of Stöber particles of similar size.[12-14, 23] Also, a change in inflammatory gene expression in response to short term exposure to SNPs has been reported.[24, 25] While these studies point to the influence of physicochemical properties of SNPs on short term toxicity (less than 10 days), their effects on subchronic (more than 90 days) and chronic toxicity and inflammation have not been investigated in detail.[18] In addition to the limited understanding of the duration of toxicity post intravenous administration, information regarding the influence of mouse's sex on SNPs subchronic toxicity is not available. To fill these gaps, we investigate the toxicity of unmodified SNPs with variations in size and porosity following single dose intravenous administration in male and female BALB/c mice up to 180 days. Here, we report the finding of dose-dependent acute (10 days) and time-dependent subchronic (60 and 180 days) toxicity studies. Tissue toxicity, blood toxicity, biodistribution and mechanisms of inflammation of SNPs overtime as a function of their size and porosity were studied. To the best of our knowledge this is the first report on safety evaluation of SNPs *in vivo* up to 180

days. Results of this study can aid in establishing guidelines for safe and effective use of SNPs in controlled delivery and other biomedical applications.

2. Materials and Methods:

2.1. Materials.

Cetyltrimethylammonium bromide (CTAB, ≥99.0%) and tetraethyl orthosilicate (TEOS, ≥98.0%) were obtained from Sigma-Aldrich (St. Louis, MO). Ammonium hydroxide (NH_4OH, 28–30% as NH_3) and absolute ethanol (200 proof) were obtained from EMD Millipore Corporation (Billerica, MA) and Decon Laboratories, Inc. (King of Prussia, PA), respectively. Limulus Amebocyte Lysate (LAL) assay kit was acquired from Lonza (Walkersville, MD). Hydrochloric acid (ACS-grade BDH, 36.5–38.0%) and phosphate buffered saline (PBS) biotechnology grade tablets were received from VWR (Radnor, PA). Neutral buffered formalin (10%), BD Vacutainer® Blood Collecting Tubes (sodium Heparin and K_2 EDTA, 3.6 mg), 31 G and 28 G syringes were all purchased from VWR (Radnor, PA). Floriso (Isoflurane) was purchased from VetOne® (ID, USA). GOT/AST and Pre-Surgical S-Panel were obtained from Heska Corporation (Loveland, CO, USA). FUJI Plain Tubes (1.5 mL) (designed for FUJI DRI-CHEM Analyzer) were received from FUJIFILM Corporation (Minato-ku, Tokyo, Japan). Tissue processing/embedding cassette was purchased from Simport, Canada. Envigo 2920X and Trizol solution were obtained from Thermofisher Scientific, USA.

2.2. Methods.

2.2.1. Silica Nanoparticle Synthesis and Characterization.—SNPs were synthesized and characterized as described previously.[24, 26, 27] A modified Stöber method was utilized to synthesize uniform spherical amorphous nonporous SNPs. The modified Stöber approach permits consistent, facile, and reproducible synthesis of uniform size spherical SNPs ranging from less than 50 nm to 2 microns. Nonporous spherical SNPs of 46 ± 4.9 nm in diameter with −40.3 ± 1.9 mV zeta potential (Stöber SNPs50) and nonporous SNPs 432 ± 18.7 nm in diameter with −53.1 ± 1.5 mV zeta potential (Stöber SNPs500) were synthesized as reported previously[24, 26] to evaluate the influence of size on subchronic *in vivo* toxicity. In order to investigate the role of porosity, mesoporous SNPs of 466 ± 86 in diameter with −44 ± 0.8 mV zeta potential were prepared using CTAB as templating agent. All SNPs were synthesized and stored in ethanol at room temperature for further experiments.

2.2.2. Animals.—Inbred BALB/c mice were used for this study. This strain of mice has an intact immune system and is genetically defined which makes it more stable, uniform and repeatable for evaluation of gene expression. Female and male Balb/c mice (43-49 days old) weighing 17.06 ± 0.6 mg and 21.35 ± 1 mg, respectively, were purchased from Charles River Laboratories (strain code #082) (3-5 mice per cage). All mice were acclimated in the animal facility for one week prior to initiating experiments and were maintained under 72-74°F and 20% humidity, subjected to 12 hr light/dark cycle with free access to food (2029X) and water. All procedures were approved by the University of Utah Institutional Animal Care and Use Committee (IACUC).

2.2.3. Intravenous Administration of Nanoparticles.—The cages were randomly assigned to treatment and control groups. Mice in each cage were weighed and randomly numbered. The number of mice per treatment group was as follows: 10-day study (5 mice/SNP/sex); 60-day study (6 mice/SNP/sex); and 180-day study (7 mice/SNP/sex). The mice were injected intravenously with freshly prepared SNPs suspended in sterile normal saline. The calculated volume of SNPs (in sterile water) was added to the concentrated saline solution (5X) in sterile water to have a desired dose of SNPs based on the average body weight of mice in each group in 0.9% saline solution (Equation 1, Table S1). The SNP suspension was sonicated and immediately injected slowly via the tail vein in a 150 μL suspension per mouse using 28 G needle syringes while monitoring the clearance of the suspension through the vein. The standard deviation in injected doses is because of the deviation in the weight of mice in each group. The right or left lateral tail veins was selected randomly for each mouse. Sterile saline (0.9%) was prepared from concentrated saline solution and sterile water and administered to control mice at equivalent volumes for each treatment group.

2.2.4. MTD Investigation.—To evaluate the MTD for each nanoparticle, different doses of nanoparticles were administered to 3-5 mice/sex/SNP. The selected number of mice was based on the initial reaction of the mouse after administration. Some mice (one or more) showed the onset of major adverse reactions even before the five mice in the same group were all injected. When this occurred, no additional mice were injected, and, thus, there were fewer than five mice in the treatment group. All mice were observed for death or clinical signs of toxicity hourly up to 12 hr and twice daily, thereafter. Any major adverse reactions such as piloerection, hunched posture, loss of weight, squinted eyes, ocular discharge, paralysis, dehydration, limping, sluggish movements, rough hair coat, slow movements, no eating or drinking, not well groomed, awkward gait, conjunctivitis, or blindness were reported as morbidity. The animals with major adverse reactions were sacrificed humanly. If the dose was reduced to a level that no such major toxicity was observed in all five mice in the group for 10 days, then this dose was identified as the MTD for 10-day post intravenous administration. Histological evidence of organ damage and abnormal values of hematological/blood chemical indices, organ weight ratios, were not considered as evidence of major toxicity in mice for determination of the MTD. Mice that survived were anesthetized by 5% isoflurane at the end of 10 days, and the blood was collected followed by euthanasia and tissue collection.

2.2.5. Animal Behavior and Body Weight.—The individual behavioral reaction to single-dose administration of SNPs at the MTD was assessed daily up to 10 days, 3 times per week up to 60 days and weekly after that up to 180 days. Mice were monitored for general behavior and signs of distress or discomfort including gait, posture, viability, movement, fur changes, bleeding, diarrhea, vocalization, self-harm, isolation from the group, activity levels, aggressiveness, porphyrin staining around the eyes and nostrils, and respiratory distress. The body weights of the mice were recorded daily up to 10 days, weekly up to 60 days and twice per month thereafter using the Compact Scale (OHAUS, VWR, USA).

2.2.6. Necropsy and Organ Weight Measurement.—Necropsy was performed on moribund mice, on mice that died, and on mice that were sacrificed after 10 days, 60 days and 180 days post injection. Following administration of inhalant isoflurane (5%) using vaporizer (Vetequip, CA, USA), the mice were sacrificed by exsanguination. The external surfaces of all organs in the thoracic, cranial cavity and abdominal cavities were examined. Vital organs including heart, liver, spleen, lung, brain, kidney, and reproductive organs (uterus and ovarian for female and testis for male mice) were extracted and weighed post-necropsy. Tissues were collected from all mice, frozen in liquid nitrogen immediately and kept at −80°C for RNA extraction or preserved in formalin for histopathological examination. The absolute and relative (organ-to-body-weight ratio) weights of the major organs were determined (Equation 2, Table S1).

2.2.7. Hematology and Blood Chemistry.—Blood was withdrawn from the hearts of mice under anesthesia using 31 G needle syringes. The collected blood was added to heparin and EDTA-coated blood collection tubes for blood cell count and blood chemistry, respectively. The blood cell counts were measured within five hr following collection. Hematological parameters included red blood cell (RBC) count and red blood cell distribution width (RDW), white blood cell count including neutrophils (NEU), lymphocytes (LYM), eosinophil (EOS), monocyte (MONO) and basophil (BAS) count, platelet (PLT) count and mean platelet volume (MPV), mean corpuscular hemoglobin (MCH) and mean corpuscular hemoglobin concentration (MCHC), hemoglobin (HGB), hematocrit (GCT) level and hemoglobin distribution width (HDW). All hematology parameters in the blood samples were determined using the CBC-HT5 Instrument (Heska, Loveland, CO, USA). For blood chemistry analyses, blood samples were briefly centrifuged at 3,000 rpm for 15 min to obtain plasma. Plasma was frozen at −80 °C and the following parameters were determined within 24 hr post collection using a DRI-CHEM veterinary blood chemistry analyzer (Heska, Loveland, CO, USA): alkaline phosphatase (ALP), alanine aminotransferase (ALT), aspartate aminotransferase (AST), blood urea nitrogen (BUN) and glucose.

2.2.8. Histopathological Examination.—Internal organs from half of the mice in each treatment group were collected at necropsy and fixed in 10% neutral buffered formalin for 3 days and kept in 70% EtOH and 4°C thereafter. The tissue processing and hematoxylin and eosin (H&E) staining were done by ARUP Laboratories (Salt Lake City, Utah). Briefly, the tissues were processed using the Tissue-Tek VIP 6 Vacuum Infiltration Processor (Sakura Finetek, CA, USA) and embedded in molten paraffin wax using the Tissue-Tek Embedding Center. The tissues were then sliced on Leica Microm RM55 Rotary Microtome (IL, USA), and placed on glass slides. The slides were stained with H&E using the Tissue-Tek Prisma Automated Slide Stainer (Sakura Finetek, CA, USA). Slides were scanned at 20X by Aperio digital pathology slide scanner (Leica Biosystems, IL, USA) and analyzed via Image Scope software (Leica Biosystems, IL, USA).

2.2.9. Tissue Preparation for Measurement of Silicon Content.—Frozen organs (liver, lung and spleen) were weighed again and thawed on ice. Cold Trizol solution was added to each vial and the tissue was homogenized using a handheld homogenizer (Omni 2000, VA, USA). Equivalent volumes of each sample were added to pre-weighed vials in

duplicate. The weight of each lysate was recorded and the samples were mixed with nitric acid (HNO_3) and kept at room temperature overnight. Then, the samples were refluxed at 95°C for 2 hr and dried at 105°C. After cooling, the residues were treated with 2 mL of 0.1% hydrogen fluoride (HF) and 5% hydrochloric acid (HCl) using 10 ppb Ga as an internal standard. The digests were transferred to polystyrene autosampler tubes and silicon was measured in quadruplicate by Inductively Coupled Plasma Mass Spectrometry (ICP-MS) (Agilent 7500ce, Santa Clara, CA, USA). The silicon content in Trizol solution, water and SNPs was also measured. The percent of silicon in each organ per injection dose for each mouse was calculated after normalization to control samples (Equation 3, Table S1).

2.2.10. Tissue RNA extraction.—Total RNA was extracted using Invitrogen Trizol reagent according to the manufacturer's procedure. The rest of the homogenized tissue for silicon measurement was transferred to a new tube for RNA extraction. The lysate was centrifuged for 5 min at 12,000 xg. The supernatant was transferred to another tube and 0.2 mL chloroform was added. After 3 min incubation on ice, the samples were centrifuged for 15 min at 12,000 xg. The colorless upper aqueous phase containing RNA was transferred to a new tube and 0.5 mL of Isopropanol added, mixed and incubated for 10 min. The white RNA precipitate was separated by centrifuging for 10 min at 12,000 xg. The RNA was washed in 75% ethanol solution, dried and dissolved in RNase-DNase free water and kept at −80°C for further processing. The quantity and quality of RNA was validated by Nanodrop Spectrophotometer (ND-1000, Thermofisher Scientific, NY, USA).

2.2.11. cDNA Synthesis and Real Time PCR Analysis.—The extracted RNA was diluted in DNase-RNase free water and first-strand cDNA was generated by QuantiTect Rev. Transcription Kit (Qiagen, MD, USA) with random primers used the following procedure: 30 min at 42°C and then 5 min at 95°C with 2721 Applied Biosystems 7900HT Thermal Cycler (Thermofisher Scientific, NY, USA). Real time PCR was performed by using a RT^2 SYBR Green Fluor qPCR Mastermix kit according to manufacturer's protocol using GeneAmp 7900HT Sequence Detection System (Applied Biosystems, Foster City, CA, USA). Threshold cycle (CT) was calculated using the algorithm provided by Applied Biosystems SDS 2.4 software. mRNA levels were normalized to GAPDH mRNA levels as reference gene using ΔΔCT method (Equation 4, Table S1). The inflammation related primers were also obtained from Qiagen (MD, USA) as listed below: GAPDH, IL1, IL2, IL4, IL6, IL10, IL12, TNFα, INFγ, CSC2 and CXC2.

2.2.12. Statistical Analysis.—For all methods statistical analyses were performed with Excel 2018 software (Microsoft, USA). Student t-test was performed. Results are presented as mean ± standard deviation of at least triplicate measurements. The difference between values was considered significant at the level of $p < 0.05$.

3. Results and Discussion:

3.1. Nanoparticle Characterization.

Three different types of SNPs were prepared. Size impact was studied using spherical nonporous SNPs of two different diameters, namely 46 ± 4.9 nm (Stöber SNPs50) and 432

± 18.7 nm (Stöber SNPs500). The particles were synthesized using a modified Stöber method.[22, 24, 26-29] Effect of porosity was evaluated by preparing mesoporous spherical SNPs with average diameter of 466 ± 86 nm (MSNPs500). The particles were characterized by X-ray diffraction (XRD), transmission electron microscopy (TEM), scanning electron microscopy (SEM), Fourier-transform infrared spectroscopy (FT-IR), dynamic light scattering (DLS), zeta potential measurement, and nitrogen adsorption-desorption analysis (Table 2S, Figure 1S and Figure 2S).[27] Figure 1 shows the TEM and SEM images of synthesized particles. The 2D-hexagonal uniformly aligned mesoporous arrangement was confirmed by XRD and TEM images. Presence of pores in MSNPs increased the total surface area to 950 $m^2.g^{-1}$ compared with similar size Stöber SNPs500 with 6.8 $m^2.g^{-1}$ surface area measured by nitrogen adsorption–desorption full isotherms. Decreasing the size of nonporous SNPs from SNPs500 to SNPs50 increased the surface area from 6.8 $m^2.g^{-1}$ to 186 $m^2.g^{-1}$. FT-IR spectra confirmed CTAB removal from mesoporous particles. Zeta potential measurements revealed negative charge (<−40 mV) in aqueous medium. Endotoxin contamination of synthesized SNPs at 1 $mg.mL^{-1}$ was assessed by end point chromogenic Limulus Amebocyte Lysate (LAL) test. The soluble endotoxin content for all prepared SNPs was less than the FDA-mandated limits (0.5 $EU.mL^{-1}$).[27]

3.2. MTD Investigation, Clinical Observation and Body Weight.

This study was designed to investigate the MTD after 10 days for each nanoparticle, followed by administration of the MTD dose, observation and analysis for up to 180 days. Various injected doses and the mortality and morbidity observations with the detailed record of adverse reactions are summarized in Tables 1 and 2, respectively.

Different SNPs were administered via tail vein to female and male inbred BALB/c mice at the dose range between 40 and 700 $mg.kg^{-1}$. The group of mice that received Stöber SNPs50 at high doses (♀141 ± 8 $mg.kg^{-1}$ and ♂153 ± 3 $mg.kg^{-1}$) showed signs of moderate pain such as hunched posture, rough hair coat, slow movements and separation from the group on the day of intravenous administration (day 0) (Table 2). At this dose, the survival percent was 43% and 50% for female and male mice, respectively, (Figure 3) with the observation that one of the male mice lost weight up to 11% before death (Table 1 and Figure 2). The rest of the mice looked normal after day 2 post-injection and 100% survived up to 10 days without morbidity (Figure 3). Two groups of five mice of each sex were injected with a lower dose of approximately 100 $mg.kg^{-1}$. These mice did not show any mortality or adverse reactions and had normal weight gain up to 10 days post-injection (Figure 2). To ensure the injection of correct safe dose, another group was injected with a lower dose (69 ± 4 $mg.kg^{-1}$) and these mice showed no signs of morbidity (Table 1 and Figure 2). Therefore, the MTD dose for Stöber SNPs50 was selected as 100 $mg.kg^{-1}$ for both female and male mice (Table 1).

All the females that received a high dose of MSNPs500 (389 ± 14 $mg.kg^{-1}$) showed 5-10% loss of weight in the first 24 hr post-injection (Table 2 and Figure 2) with moderate signs of pain, and died after 48 hr. Since this dose was too toxic, it was not injected into the males. The second selected dose (♀208 ± 7 and ♂200 ± 13 $mg.kg^{-1}$) was administrated to both sexes (Table 2). Some of the females and males showed moderate signs of pain (Table 2) and

the survival percent was 67% and 50% for female and male, respectively (Figure 3). The injected dose was further decreased, in the groups of 5 mice/sex that were injected with approximately 100 $mg.kg^{-1}$ of MSNPs500 to females and 40 $mg.kg^{-1}$ to males, all the mice survived up to 10 days without any signs of pain or morbidity. Therefore, this dose was reported as MTD for mesoporous nanoparticles (Table 1). The dose dependent toxicity of MSNPs in 11 female and 19 male mice showed considerable systemic sex-related toxicity, with MTDs ranging from 40 ± 2 $mg.kg^{-1}$ to 95 ± 2 $mg.kg^{-1}$ for male and female mice, respectively. This toxicity was influenced by porosity of SNPs where Stöber SNPs with the same size did not show the same effect. All of the SNPs were injected on the same day for both sexes of BALB/c mice. Mice were the same age and about the same weight. Earlier studies suggested that the sex-associated hormones indirectly or directly influence Th2 or Th1 cell activation. Therefore, the immune response in animal models, such as BALB/c mice, may have contributed to the toxicity.[30-32] The data shown here demonstrate the importance of studying sex-related toxicity of SNPs. The mechanisms of such differences need further investigation.

The mice that were injected with the sequentially higher doses of Stöber SNPs500 in the range of 400-700 $mg.kg^{-1}$ showed the most severe clinical signs of toxicity among the particles studied (Tables 1 and 2). The survival rate of these mice decreased to 60% and 33% for males (479.39 ± 39 $mg.kg^{-1}$) and for females (707 ± 14 $mg.kg^{-1}$), respectively (Figure 3). Relative to mesoporous particles of the same size (MSNPs500) the time of death for these mice decreased to 24 hr. Affected mice showed signs of severe pain such as violent reaction to stimuli or when approached with ataxia, changes in respiration, necrosis at the end of tail, limping, paralysis of hind legs or hemiplegia (Table 2). Due to these symptoms, the third administered dose was at 377 ± 6 $mg.kg^{-1}$ and 392± 12 $mg.kg^{-1}$ for females and males, respectively. All the mice in these groups survived. However, signs of weakness, blindness and loss of weight up to 24% were observed at this dose (Figure 1). The last group of mice was injected with ~300 $mg.kg^{-1}$ of Stöber SNPs500. All 5 mice of both sexes looked healthy during the 10 days of the experiment (Table 1 and Figure 3). Accordingly, the dose of 300 $mg.kg^{-1}$ was chosen as the MTD for Stöber SNPs500.

Overall, our observations showed that the 10-day maximum tolerated dose of smaller particles (Stöber SNPs50 nm) is less than that of larger particles (Stöber SNPs500). The mesoporous particles (MSNPS500) were more toxic than their nonporous counterparts (Stöber SNPs500) (Table 1). We previously reported the same trend for different sizes of SNPs in CD-1 mice.[12-14] We showed that Stöber SNPs (115 and 170 nm) compared to MSNPs of comparable size (120 and 208 nm) had MTDs of 450 $mg.kg^{-1}$ and 30 $mg.kg^{-1}$ in female CD-1 mice, respectively.[12, 14] The MTD for Stöber SNPs50 in BALB/c mice was 100 $mg.kg^{-1}$. However, the same size of SNPs showed MTD of 200 $mg.kg^{-1}$ in CD-1 mice. Assuming that there were no differences between various batches of SNPs, it is also plausible to suggest that the toxicity of SNPs may be mouse-strain related.

We further found that during short-term systemic exposure, toxicity appears to be more severe when larger particles (Stöber SNPs500) are administered intravenously. Based on the toxicity symptoms such as paralysis, blindness, shortness of breath and weakness we suggest that coating/surface instability and aggregation upon administration of these non-surface

modified particles following obstruction of blood capillaries may serve as a potential underlying reason for the toxicity of Stöber SNPs500 in this study. In addition to the clinical observation, the time of death was also influenced by the type of particles studied. At the toxic dose, nonporous Stöber SNPs, irrespective of their size, dose and sex, resulted in mouse death during the first 24 hr following injection. But, toxic doses of MSNPs500 required 1-3 days for death to occur in female and male BALB/c mice. The reason for this difference is unclear. On the other hand, toxic doses of SNPs50 and MSNPs500 caused moderate morbidity in comparison to larger SNPs500 in the mice prior to their death. This could be because of relatively higher injection dose of the larger nonporous Stöber SNPs500. Further studies are needed to test this hypothesis.

For subchronic studies, another series of mice were assigned for two time points of the study, *i.e.*, for 60 days and 180 days. These mice (SNPs/sex) were injected on the same day with the average MTD doses of 100 $mg.kg^{-1}$ for SNPs50 nm, and 300 $mg.kg^{-1}$ for SNPs500. To keep the injection dose the same and to compare both sexes based on the amount of injected silicon, the MSNPs were also injected at a higher MTD for females (100 $mg.kg^{-1}$). Mean body weight of each group is shown in Figure 1. Treatment with MTD of SNPs did not cause any adverse effect on mouse behavior and growth during the 180 days post single dose intravenous injection (Table 2 and Figure 1). Our results are consistent with other reports of intravenous administration of smaller SNPs (10 and 13 nm) to Sprague-Dawley rats for up to 60 days [33], PEGylated and non-PEGylated mesoporous silica nanoparticles (80-360 nm) to male ICR mice for one month,[34] ORMOSIL MSNPs (20-25nm) to female athymic nude mice for 15 days,[35] 13 nm MSNPs and Stöber SNPs (70nm) to male Wistar rats and male BALB/c mice, respectively for 60 days. [33, 36] Therefore, as we will discuss below, our results are consistent with these studies showing that even though SNPs do not show any subchronic abnormal clinical observation, they do cause tissue toxicity, blood toxicity and inflammatory response over time.

3.3. Necropsy Findings and Organ Weight Measurement.

At the end of each time point, all surviving mice were sacrificed. Gross tissue injuries were mostly found in mice that were injected with SNPs500). One mouse that was administered Stöber SNPs500 (707 ± 14 $mg.kg^{-1}$), became blind and was paralyzed in 10 days (described above in Section 3-2). White tissue discoloration was observed grossly in the left hemisphere of the brain which was attributed to the inflammation secondary to infarction. Also, the vitreous body of the right eye was pale which was likely caused by altered blood supply. Gross tissue damage was also observed in a mouse that was administrated with Stöber SNPs500 (381.85 $mg.kg^{-1}$). Similar brain injury was also seen in two mice (one male and one female) that received MTD of Stöber SNPs500 and survived for 60 days. Overall findings suggested that infarctions occurred early after the injections and while some animals recovered clinically over time, tissue damage persisted. Weights of various organs among male and female mice were not significantly different in comparison to the control group (Figure 4). No significant changes in the organ weights of the mice administered with Stöber SNPs50, Stöber SNPs500 or MSNPs500 were observed following acute and subchronic exposure.

3.4. Hematology and Blood Biochemical Examination.

To investigate the impact of SNPs on blood toxicity over time, blood was collected via heart puncture of surviving mice on days 10, 60 and 180 post-injection. The results of blood cell counts and blood chemistry analyses are shown in Tables 3 and 4.

The results show a significant change in platelet, MCHC and white blood cells 10 days and 60 days post intravenous injection of SNPs. As shown in Table 3, significant differences was observed in the mean corpuscular hemoglobin (MCHC) and platelet values for all the mice that were injected with SNPs and survived for 10 days, except the females that received a MTD of MSNPs. Among these mice, the female and male mice that received a MTD or higher of Stöber SNPs500, also showed significant increase in platelet volume. Mean corpuscular hemoglobin concentration measures the concentration of hemoglobin in a specific volume of blood and is calculated by dividing the hemoglobin by the hematocrit.[37] As we reported the hemolytic activity of SNPs previously,[38] the high MCHC values in these mice might occur because the red blood cells become fragile and are lysed after SNPs administration. This effect lasts for 60 days in the mice that received smaller doses of SNPs (Table 3). This red blood lysis also results in lower hematocrit value which is defined as a percentage of red blood cells in total blood volume. The signs of thrombosis are related to tissue damage and capillary occlusion by aggregated particles. The damage by the aggregates happens first and results in blood loss, which in turn would consume coagulation factors, which later may lead to hemorrhage with a subsequent decrease in hemoglobin and hematocrit. An increase in the platelet count serves as body's defense mechanism against tissue damage and blood loss. An increased platelet count at day 10 post intravenous injection, is also correlated with tissue damage and associated bleeding or blood clotting. Our observation of decreases in HGB and HCT, is further correlated with tissue damage and blood loss at earlier time points that was confirmed by hematology results. The smaller size of Stöber SNPs50 causes significant increase in red blood cell distribution width (RDW) irrespective of the injected dose. This phenomenon may also be due to anemia that occurred following acute exposure to the smaller Stöber SNPs50. WBC counts, including monocyte, lymphocyte and neutrophil counts decreased in the mice injected with MSNPs at different doses during the 10 day period (Table 3). The data also shows that this parameter further decreased (in more than 50% of mice) 60 days after single dose intravenous administration of Stöber SNPs500 and MSNPs500 (Table 3). Neutrophils and monocytes are inflammatory cells with phagocytic functions. They participate in tissue repair after infarctions and they may also phagocytize the particles to facilitate detoxification process. Nevertheless, the decrease in this cell type may be due to the direct toxicity of particles to neutrophils or the ongoing inflammatory process. When activated, these cells are redistributed to the damaged sites, so the decrease in peripheral blood is likely temporary, and the number of cells is usually restored as soon as the inflammation is resolved (180 days post injection) (Table 3). A decrease in lymphocytes may also be due to the direct toxicity of particles to the lymphocytes. It further suggests spleen tissue damage at earlier time points that was confirmed by hematology observations. Since we measured the total count and not the differential count, we cannot say which type of lymphocytes were affected. If we follow the same logic with lymphocytes as with monocytes and neutrophils (*i.e.*, uptake and direct toxicity to the cells), then likely, the B-cells are affected by SNPs, because these cells are

also phagocytic and can take up particulates. The long-term and more severe subchronic decrease in the number of WBCs in 70-100% of injected mice with large SNPs (SNPs500 and MSNPs500) could reflect the possible severe damage to bone marrow. The suppression of bone marrow in the presence of large SNPs could slow recovery of new WBC and therefore subacute decreases in their numbers in peripheral blood 60 days after administration. On the other hand, higher amounts of NPs or larger NPs can be more toxic for macrophages *in vivo*. For example, lysosomal dysfunction might occur as a result of cellular accumulation of silica NPs that could produce ROS in macrophages.[39] This effect seems reversible, since we did not observe any reduction of WBC counts in the animals on day 180.

After 60 days, both sexes that were injected with Stöber SNPs500 as well as the female mice injected with Stöber SNPs50 showed significant decreases of hematocrit which suggests anemia still remains in these treatment groups. However, this was recovered in the MSNPs500 treated group. Female mice that received Stöber SNPs500 showed higher platelet values (Table 3). Since the same results were found in female control groups, these changes were not considered significant. The same changes were seen at the 180-day study in all groups besides the controls. The rest of the blood parameters were normal 180 days post injection. It can be concluded that there was not any persistent measurable toxicity as seen by blood cell parameters for single dose intravenous exposure to SNPs.

The data presented here show the 10-day acute and 60-day subchronic blood toxicity of SNPs. Most of the toxicity that we have observed is due to the direct toxicity of the SNPs to the RBC and WBC, which could be due to hemolysis and phagocytosis of the SNPs. Perhaps the important data here is the significant time-dependent increases in the blood phagocytic activity by monocytes and neutrophils in MSNPs500 treated mice. It appears that these particles phagocytose more or faster, or even have longer blood circulation times in comparison with the same size but nonporous Stöber SNPs500. This may explain the reason for the increased *in vivo* toxicity of mesoporous particles we observed compared to the *in vitro* conditions as well as delay in time of death in the presence of MSNPs500.

As shown in Table 4, all the mice that survived showed a normal range of values for alkaline phosphatase (ALP), alanine aminotransferase (ALT), aspartate aminotransferase (AST), blood urea nitrogen (BUN) and glucose at 10, 60 and 180 days post injection (Table 4). This data confirms that single doses of SNPs administered in this study do not have toxicity on serum parameters of female and male BALB/c mice.

3.5. Histology.

The potential toxicity of SNPs after short- and long-term intravenous exposure (10 to 180 days) was further evaluated by histological examination of the major organs including liver, lung, brain, spleen, heart, kidney, eye and reproductive organs (uterus and testis). The histology findings of affected organs from animals treated with high dose and in the recovery groups for toxic dose in 10-day study, and experimental group at the MTD for 10-day, 60-day and 180-day exposure are summarized in Table 5, and Figures 5-8. To avoid presenting the same data, only representative histologic lesions from each tissue are displayed in the figures. We focus the discussion on the selected mouse tissue that exhibited

a major adverse reaction post intravenous administration of SNPs at a toxic dose and a MTD over time. The mice that received a high dose (>MTD) of smaller Stöber SNPs50 showed foci of lobular inflammation within the liver with aggregates of foamy histocytes in the spleen. There were no histopathologic abnormalities observed in other organs, except for the lungs recovered from male mice receiving 149 $mg.kg^{-1}$ which showed thrombosis in one of the main vessels. As expected, the clearance organs, liver and spleen, are the targeted organs for small Stöber SNPs50 toxicity.

When compared with control mice that received saline, majority of the mice treated with MSNPs500 at a high dose (>MTD), developed small foci of lobular inflammation and ceroid laden macrophages in liver, also massive thrombosis in the pulmonary vessels with or without foamy histocytes (Figure 5 a-d), which were observed in three out of six mice. Female or male mice that received ~400-500 $mg.kg^{-1}$ MSNPs, showed scattered foamy macrophages within the spleen. There was a wedge shaped injury of the renal parenchyma within the kidneys in four of six female mice which showed focal wedge shaped tubular damage with variable calcifications in keeping with infarctions (Figure 5 e, f). Figure 5 shows the liver, heart and eye of male mice that received MSNPs500 (526.04 $mg.kg^{-1}$) demonstrating small foci of lobular inflammation and ceroid laden macrophages in the liver, focal calcified myocytes and focal subretinal calcification in one of the eyes.

The major clinical adverse reaction, observed in our study was induced by a toxic dose of Stöber SNPs500. Observations with Stöber SNPs500 as described in Section 3-2, correlated with abnormalities observed in our histology analysis. The high toxic dose of Stöber SNPs500 (700 $mg.kg^{-1}$) caused death in two of three mice. The mouse that survived became blind (right eye) during the 5 days post-injection (see Section 3-2) and also developed paralysis. Histopathologic evaluation revealed an organizing infarction in the left hemisphere of the brain (see Section 3-3) with inflammatory infiltrate composed of histocytes and lymphocytes (Figure 6 g,h). The right eye showed calcifications and mixed inflammatory infiltrate in keeping with probable infarction (Figure 6 i). The heart showed focal necrotic myocytes with calcifications (Figure 6 f). There was focal wedge shaped tubular damage with associated calcifications in kidney in keeping with a focal infarct and organizing thrombosis in the pulmonary vessels (Figure 6 d,e). Brain and kidney infarcts were also found in another female animal which received a lower dose of Stöber SNPs500 (400 $mg.kg^{-1}$). The rest of the females and males in this group showed thrombosis in at least one vessel of the lung (Figure 6a,b,c), small foci of lobular inflammation and ceroid laden macrophages in the liver and aggregation of foamy histocytes in the spleen. Our data show time-, size- and porosity-dependent tissue acute toxicity in liver, spleen, lung, kidney, eye, heart and brain post intravenous injection of SNPs. Based on the type of lesions, aggregation of SNPs or clotting the blood stream after intravenous injection might cause the major infarction and thrombosis organization that have been seen in most of the mice who received high dose injections of SNPs. Aggregation of vacuolated or foamy macrophages in the liver and spleen could indicate nanoparticle uptake by macrophages which could be a sign of the body's effort for detoxification and clearance. Presence of inflammation and calcifications is an expected part of a late tissue repair mechanism, which occurs after infarctions or injury caused by NPs. Additionally, this tissue toxicity correlated with silicon accumulation in these organs (discussed in Section 3-6). Although, the particles tested negative for the LAL

assay, this assay detects only free endotoxin. Therefore, we cannot exclude potential presence of endotoxin in the cavities (pores) of MSNPs, which are invisible to the LAL. If this endotoxin is released *in vivo*, it may contribute to the inflammation. Such dissociation would not invalidate our study, because porous materials are known for difficulties with accurate endotoxin quantification.

The Larger Stöber SNPs did induce subchronic tissue toxicity at the MTD of 300 mg.kg^{-1}) 60 days post intravenous injection. Two mice (one female and one male) had early infarctions in their brain that were also observed after necropsy (Section 3-3). Foci of chronic lobular inflammation with aggregation of macrophages and neutrophils were observed in the liver of all the mice in this group which were preserved during histological examination. Two out of five mice also showed organized thrombi in pulmonary vessels and aggregates of macrophages with or without neutrophils in the spleen, 60 days after Stöber SNPs50 and Stöber SNPs500 intravenous injection (Figure 7 a, b). No significant abnormalities were identified microscopically in the organs recovered from mice receiving the same size SNPs, but mesoporous SNPs (MSNPs500), 60 days after injection. A focal injury of the brain tissue with necrosis, macrophages and calcifications, likely representing a small infarction was observed in the brain of one of the female mice that received the MTD of Stöber SNPs500. These results show the effect of size and porosity on 60 day subchronic tissue toxicity of SNPs. As it is summarized in Table 5, after 60 days, mice injected with Stöber SNPs500, the liver, spleen and lung were being cleared of SNPs. With same size mesoporous SNPs (MSNPs500), the spleen and lung had recovered at day-60 post injection. Such long-term recovery process also could be because of lower amount (in mg) of MSNPs500 that were injected into the mice (compare MTDs). Interestingly, although MSNPs500 caused more and longer toxicity in the phagocytic systems (see blood toxicity results), the 60-day tissue subchronic toxicity of these particles is less than that of nonporous ones. We can compare our data with some studies using SNPs of different sizes, surface characterization and time of exposure. For example, He and coworkers have reported the safety of PEGylated and non-PEGylated mesoporous SNPs (80-360nm) over a period of one month upon single dose intravenous administration.[34] Their data showed MSNPs and PEGylated MSNPs of different particle sizes accumulate mainly in the liver and spleen, a minority of them in the lungs, kidney and heart. Neither MSNPs nor PEGylated MSNs cause tissue toxicity 1 month after injection. The subchronic liver and spleen injuries was reported up to 60 days after chronic intravenous infusion of 13 nm MSNPs and Stöber SNPs (70 nm) to male Wistar rats and male BALB/c mice, respectively.[33, 36]

After 180 days, the mice from the same dose treatment group (MTD) did not induce obvious pathologic lesions as measured by the tissue morphology from these mice was found to be similar to that of normal mice in the control group (Figure 8). A very focal lobular inflammation in the liver was also observed in a subset of mice in the control groups. There was also one mouse with focal hemosiderin deposition within the spleen with unknown clinical significance, because the same morphology was observed in saline injected mice and hemosiderin formation usually happens in mice as they age. MSNPs500 did not induce obvious pathologic lesions in most of the mice during the 60-day study, except for macrovascular in the liver of one male mouse and a focal hemosiderin deposition in two female mice out of 4 mice (Figure 8). Our results presented here show that Stöber SNPs500

after 180 days post intravenous injection showed more severe tissue damage relative to the other SNPs. The most important pathological changes in this group occurred in the liver and spleen which was thrombosis along with calcification within the pulmonary vasculature (Figure 8a), small aggregates of mostly lobular inflammation composed of admixed lymphocytes and ceroid laden macrophages, and mild macrovesicular steatosis within the liver tissue (Figure 8b-d). Figure 8, e-g also shows aggregates of foamy histocytes with admixed neutrophils found in the spleen, and focal splenic hemosiderin deposition in some of the mice. One case of a male mouse injected with 312.15 $mg.kg^{-1}$ of Stöber SNPs500 showed focal calcification in the heart. In addition, one female animal injected with a 346.19 $mg.kg^{-1}$ dose, also had thrombus within the heart (Figure 8h,i). Microscopic changes in liver and spleen of this group were randomly distributed among different groups and within the range of normal background lesions. These results show that at 180 days post single dose intravenous administration of the nanoparticles, subchronic tissue toxicity of SNPs is influenced by the size of the particles. Liver and spleen recovery by the mice administered the larger Stöber SNPs500 took a longer period (180 days) compared to smaller Stöber SNPs50.

The summary of tissue toxicity of SNPs is listed in Table 5. Our results show size and porosity-dependent liver, spleen and lung acute and subchronic toxicity of SNPs. Interestingly, although smaller particles (Stöber SNPs50) are more toxic *in vivo*, the subchronic toxicity of these nanoparticles seems less and the recovery process from the smaller SNPs (Stöber SNPs50) is faster. Also, the same trend was observed for mesoporous SNPs (MSNPs500).

Our results demonstrate that the nanoparticles studied have not shown severe subchronic tissue toxicity after a single dose intravenous injection. Most of the lesions which were seen in 60 days and 180 days of the study, are related to the recovery and clearance process of the body after blood obstructions and macrophage uptake. However, this process is dependent on size and porosity of SNPs. The larger Stöber SNPs500, that were injected with a larger quantity of SNPs (higher MTD), need 180 days to recover from tissue injury, but mice with the same size but porous nanoparticles (MSNPs 500nm), and similar to smaller particles (Stöber SNPs50) recovered in 60 days post injection. Our results are comparable to the acute and subchronic studies of SNPs (different size) on other animal strains which were studied for a shorter time period (10 days and 4 weeks). For example, Nishimori and coworkers reported liver and spleen as major injured organs for toxicity of 70 nm SNPs at 4 weeks in male BALB/c mice intravenously.[36] Yu and coworkers have also seen liver, lung and spleen damage in female and male ICR mice 14 days after single intravenous injection of lethal doses of amorphous SNPs.[40]

3.6. Silicon Accumulation Measurement in Injured Organs.

Since liver, lung and spleen were the most affected organs after acute and subchronic exposure to different SNPs at the MTDs, we measured the silicon content in these tissues to see if there was still SNPs or their dissolution products in these tissues over time. The silicon content of each organ of 3 mice was measured by ICP-MS and the percentage of silicon per injection dose to each animal was calculated (Table S1). Figure 9 shows the values after

normalization to control samples (saline-injected mice). Since the MTD value for Stöber SNPs500 was more than the other SNPs, (300 *vs* 100 $mg.kg^{-1}$), the silicon content in the mice that received these SNPs was more than the others (Figure 10). Relative to lung, significant increases in silicon levels were noted in liver and spleen of all three different SNPs treatment groups 10 days and 60 days post injection. At day 180 after injection, the silicon amount in all mice was negligible which means the dissolution products were cleared from these tissues. The results of silicon content measurements suggest that the smaller SNP, Stöber SNPs50 accumulated silicon to the same extent in liver and spleen 10 days post injection. This distribution significantly changed after 60 days, where spleen had less silicon content than the liver. Stöber SNPs500 showed an opposite pattern. For these particles the accumulation after 10 days was more pronounced in the liver than in spleen. For Stöber SNPs500, after 60 days these two organs showed the same amount of silicon. MSNPs500 showed the same trend of accumulation. The liver had more silicon than spleen 10 days and 60 days after injection, whereas at 180 days, no accumulated silicon was observed. Based on current observations, it appears that SNP accumulation in the liver, lung and spleen was dependent on particle size at 10 days. Regardless of their porosity, at 10 days, larger particles, Stöber SNPs500 and MSNPs500, accumulated in the liver to a higher extent than spleen and in spleen larger particles accumulated to a higher extent than in the lung. For smaller particles, Stöber SNPs50, accumulation in liver and spleen was equal. Previous studies also reported liver and spleen as target organs both after single and repeated intravenous exposure to SNPs.[41] Our results are consistent with other reports that showed smaller (13nm) mesoporous silica nanoparticles were conspicuously retained in the liver of male rats for up to 60 days.[42] Kumar *et al.* also showed more accumulation of modified MSNPs (ORMOSIL)(20-25nm) in spleen, liver, and stomach than in kidney, heart, and lungs after intravenous injection. The authors suggested clearance of MSNPs via the hepatobiliary excretion over a period of 15 days without any adverse effect or any other abnormalities in the selected tissues.[35] Although, based on the data here, we cannot conclude how long SNPs stay intact in the body, it is possible that SNPs and/or their degradation products may remain in the mice tissues up to 60 days post injection and cause blood, lung, liver and spleen subchronic toxicity. Subchronic distribution of these particles in these tissues over time also depended on physiochemical properties. The silicon concentration decreased significantly in spleen of mice injected with smaller Stöber SNPs50 and mesoporous SNPs, MSNPs500, between 10 and 60 days. For Stöber SNPs500 an opposite trend was observed, but the effect was not significant. This could be due to the longer process of clearance of the larger Stöber SNPs from the liver due to reduced surface area.[41] Since most of the SNPs accumulated in liver and spleen, it is possible that the nanoparticles are either taken up by phagocytic cells in the blood or accumulated in liver and spleen resident macrophages for further clearance. This long-term silica nanoparticle stability in macrophages was reported before.[43] Xie *at al.*, observed that a significant number of SNPs remain in liver and spleen 30 days post intravenous administration of 10 $mg.kg^{-1}$ to ICR mice.[43] They hypothesized that silica nanoparticles can accumulate in macrophages and resist rapid digestion. [43] It has been reported that macrophages can uptake and compartmentalize silica NPs up to a certain concentration threshold. At this threshold the cells are no longer able to handle nanoparticle internalization and this phenomenon is size dependent.[44] Therefore, in this study, due to relatively high mass of injected large silica NPs, the body needed minimum 60

days to produce new macrophages, collecting all the SNPs from the body and digest the particles. A lower injection dose of nanoparticles combined with increasing the frequency of intravenous administration could potentially reduce clearance time for these particles and increase the safety of SNPs upon intravenous administration. On the other hand, frequent injection could trigger some other toxicities in blood and organs. As we mentioned before, the possible bone marrow suppression effect of SNPs could be reversible. Further production of WBCs and recycling macrophages could help the body to completely recover the remaining silicon from the body between day 60 and day 180. It can be concluded that for the silica nanoparticles studied, the injected doses in this animal strain need 180 days to be completely digested.

3.7. Inflammatory Gene Expression in Organs.

To gain insight into the inflammatory response to these particles, the regulation of inflammatory cytokine gene expression as a function of time was measured by real time PCR. We analyzed the expression of genes involved in acute inflammation such as *CSF, IL-1β, IL6, Cxcr2 (IL8R), TNFα* and also the cytokines in chronic inflammation such as *IL4, IL5, IL10, IL12, INFγ*.[45] Among the genes studied, the main cell sources for interleukin *IL1, IL8*, and *TNFα* are macrophages. Colony stimulating factors (CSF2) are mostly secreted by macrophages, fibroblast and endothelial cells. The rest of interleukins, *IL4, IL5, IL6* are from T-helper cells and *IL10, IL12* and *INFγ* are secreted by activated T-cells[46]. As shown in Figure 10, except for *Csf2*, the other inflammatory cytokines were overexpressed significantly in the liver of the mice that received Stöber SNPs50 at day 60 which is because of accumulation and activation of macrophages in this tissue. It has been reported that macrophages secrete cytokines such as tumor necrosis factor (*TNF*), *IL1, IL6, IL8*, and *IL12* when they are exposed to inflammatory stimuli [47]. This overexpression of cytokine was still observed on day 180 post injection, except for two genes, *IL4* and *IL12*. The spleens of the same treatment group (Stöber SNPs50) showed downregulation or no significant changes for genes studied on days 10, 60 and 180. Lung tissue, with the least accumulation of these particles showed significant upregulation of *Cxcr2, IL6* and *IL5* on day 10. The expression of *TNFα, IL10* and *INFγ* also increased about 3-4 fold in the lungs of mice treated with Stöber SNPs50 180 days post administration. These results clearly show time dependence of the inflammation response of liver and lung after a single dose injection to BALB/c mice. An inflammatory response was observed in the liver of mice that were injected with Stöber SNPs500 to a much higher extent especially on day 60, irrespective of their porosity. As it is highlighted in heat map of Figure 10, all the cytokines studied overexpressed significantly in liver. MSNPs500 caused significant overexpression of *Csf2* and *IL1β* on day 10 and day 180. Also, *Cxr2, TNFα, IL10, IL5* and *INFγ* overexpressed about 2 to 8.5 fold in the same treatment group on day 180. A few of the inflammatory cytokines (most significantly *Csf2*, *IL5* in spleen and *Csf2*, *IL1β, TNFα, IL10, IL12, INFγ* in lung) were also overexpressed in the spleen and lung of the mice that were injected with the MTD of MSNPs. This increase occurred acutely for the spleen and mostly subchronically for lung tissue. The high overexpression of inflammatory cytokines is correlated with the increased number of lymphocytes and monocytes at day 60 following large SNP, Stöber SNPs500, injection (as describe before, Section 3-4). As our histology data also showed, Stöber SNPs500 that had the higher MTD, caused acute and 60 days

subchronic liver inflammation. Accumulation of Stöber SNPs500 in the spleen resulted in upregulation of *Csf2, IL10* and *IL12* on day 60 and *Cscr2* on day 180. Most of the cytokines studied downregulated or didn't show significant acute or subchronic changes in lung tissues of mice treated with Stöber SNPs500, except about 5 to 9 times overexpression in *IL6* on d10 and *Cscr2* on d180, respectively. The subchronic inflammation in the lung of these mice was also confirmed by slight upregulation of *IL6, TNFa, IL4* and *IL5*. Therefore, the subchronic liver and lung inflammation response of SNPs correlated to the porosity of particles.

It is likely that the particles, especially Stöber SNPs50 constructs, accumulated by phagocytic cells (monocytes and macrophages) are not toxic to these cells. Therefore, we do not see significant pro-inflammatory cytokines. Liver-resident Kupffer cells are reported as responsible for nanoparticle clearancefrom systemic circulation in mice. Stöber SNPs, especially Stöber SNPs 500, that are shown to be less toxic to macrophages[24], could be trapped by these phagocytic cells and cause upregulation of most of the cytokines studied at the subchronic time point. As discussed above, all the SNPs studied accumulated mostly in the liver up to day 60. The accumulation of SNPs in these organs correlated with the histology lesions. Results demonstrate the influence of SNPs size and porosity on subchronic inflammation response of the body in liver, lung and spleen. The inflammation may be triggered by tissue damage. Therefore, the results of this analysis are in agreement with earlier histology observation. Inflammation in response to tissue damage occurs to clear the damaged cells and promote healing. The dysregulation of such host-protection response may lead to other long-term toxicity which were not analyzed in our study.

An increase in basophils and eosinophils that was seen on day 10 and day 60 in most of our SNPs treatment groups correlates with the increase in *IL5* in the liver. *IL5* is produced by many cells, including, but not limited to, T-cells, innate lymphoid cells and endothelial cells[46]. *IL5* function is to promote the maturation and support the activation of basophils and eosinophils. Thus, the increase of these cells in the blood may be explained by the presence of *IL5. IL5* is a Th2 cytokine [48], and our study is also conducted in a Th_2-biased animal model[49]. *IL4*, another essential mediator of Th_2 differentiations[46], was also overexpressed in the liver after chronic exposure to different types of SNPs in BALB/c mice.

An interesting observation in the present study was the tissue toxicity and accumulation of SNPs in liver on day 10. They were more on day 10 than that on day 60 and much more than on day 180. However, severe inflammatory response occurred in our subchronic studies, *i.e.*, on day 60 and day 180 post-injection. One way to explain this observation is that in the first days after injection, the high concentration of SNPs caused toxicity to the macrophages that take up these particles. The surviving macrophages guide the SNPs to the clearance organs and this makes the peak of secretion of cytokines in those organs occur at a later time (in our study day 60). Almost all the particles would be cleared from these tissues by day 180, thereby decreasing the related inflammatory response. It is clear that the inflammatory response is beneficial for the host body when the cytokines are produced in appropriate amounts, but would be toxic when the cytokines are secreted in a deregulated fashion[47]. The acute inflammation response we report here is consistent with the observation that the acute severe inflammation response occurs for 100 and 200 nm SNPs 12 hr after a single

intravenous injection[47]. Additional molecular evaluations of the protein levels and activation of these cytokines, as well as the correlation of pro-inflammatory to anti-inflammatory genes, are needed to determine the *in vivo* mechanism(s) of acute and subchronic signaling pathways of SNPs.

Conclusion:

In conclusion, our results indicate distinct differences in the *in vivo* acute and subchronic blood and tissue toxicity and inflammation profiles of SNPs as a function of size, porosity, animal sex and time. Stöber SNPs50 and MSNPs500 seem to be more toxic under acute conditions. These nanoparticles showed less subchronic toxicity on days 60 and 180 at the MTD in comparison to the large, nonporous Stöber SNPs500. Male BALB/c mice appear to be more sensitive to MSNPs500 in 10 days survival evaluation, although the sex of the mice did not have a substantial influence after 60 and 180 days. Tissue toxicity and accumulation of SNPs in liver (most affected tissue) did not have the same trend. Although a severe inflammatory response occurred in the subchronic studies (day 60 and day 180), the higher accumulation of SNPs was reported on day 10 post intravenous injection. More experimental evidence will be required to determine the nanoparticles' capability to cause an immune response after intravenous administration and also the mechanisms of their long-term blood and tissue toxicity.

Supplementary Material

Refer to Web version on PubMed Central for supplementary material.

Acknowledgment:

We would like to acknowledge Dr. Lawrence McGill, veterinary pathologist in Salt Lake City for assistance in histological sample analysis, and Dr. Marina A. Dobrovolskaia from NCI Nano Characterization Laboratory, Dr. Khaled Greish from Arabian Gulf University, and Dr. Philip Moos and Dr. Christopher A. Really of the University of Utah for their detailed review and suggestions for the manuscript. The histology experiments for this study were conducted with support from the biorepository and molecular pathology shared resources supported by the grant awarded to the Huntsman Cancer Institute by the National Cancer Institute of the National Institutes of Health. The authors also acknowledge the use of the University of Utah shared facilities of the Micron Microscopy Suite and the University of Utah USTAR shared facilities supported in part by the MRSEC Program of the NSF under Award No. DMR-1121252. Financial support for this project was provided by the National Institute of Environmental Health Sciences of the NIH (R01ES024681).

References:

[1]. Nel AE, Meng H, Liu X, Mesoporous silica nanoparticles with lipid bilayer coating for cargo delivery, Google Patents, 2018.

[2]. Nel AE, Zink JI, Meng H, Lipid bilayer coated mesoporous silica nanoparticles with a high loading capacity for one or more anticancer agents, Google Patents, 2016.

[3]. Slowing II, Trewyn BG, Lin VS-Y, Mesoporous silica nanoparticles for intracellular delivery of membrane-impermeable proteins, Journal of the American Chemical Society, 129 (2007) 8845–8849. [PubMed: 17589996]

[4]. Liong M, Lu J, Tamanoi F, Zink JI, Nel A, Mesoporous silica nanoparticles for biomedical applications, Google Patents, 2018.

[5]. Trewyn BG, Slowing II, Giri S, Chen H-T, Lin VS-Y, Synthesis and functionalization of a mesoporous silica nanoparticle based on the sol–gel process and applications in controlled release, Accounts of chemical research, 40 (2007) 846–853. [PubMed: 17645305]

[6]. Meng H, Xue M, Xia T, Ji Z, Tarn DY, Zink JI, Nel AE, Use of size and a copolymer design feature to improve the biodistribution and the enhanced permeability and retention effect of doxorubicin-loaded mesoporous silica nanoparticles in a murine xenograft tumor model, ACS nano, 5 (2011)4131–4144. [PubMed: 21524062]

[7]. Zhou Y, Quan G, Wu Q, Zhang X, Niu B, Wu B, Huang Y, Pan X, Wu C, Mesoporous silica nanoparticles for drug and gene delivery, Acta pharmaceutica sinica B, (2018).

[8]. Caltagirone C, Bettoschi A, Garau A, Montis R, Silica-based nanoparticles: a versatile tool for the development of efficient imaging agents, Chemical Society Reviews, 44 (2015) 4645–4671. [PubMed: 25406516]

[9]. Parasuraman S, Toxicological screening, Journal of pharmacology & pharmacotherapeutics, 2 (2011) 74. [PubMed: 21772764]

[10]. https://ntp.niehs.nih.gov/testing/types/cartox/index.html.

[11]. Greish K, Thiagarajan G, Ghandehari H, In vivo methods of nanotoxicology, Nanotoxicity, Springer, (2012) 235–253.

[12]. Greish K, Thiagarajan G, Herd H, Price R, Bauer H, Hubbard D, Burckle A, Sadekar S, Yu T, Anwar A, Size and surface charge significantly influence the toxicity of silica and dendritic nanoparticles, Nanotoxicology, 6 (2012) 713–723. [PubMed: 21793770]

[13]. Yu T, Greish K, McGill LD, Ray A, Ghandehari H, Influence of geometry, porosity, and surface characteristics of silica nanoparticles on acute toxicity: their vasculature effect and tolerance threshold, ACS nano, 6 (2012) 2289–2301. [PubMed: 22364198]

[14]. Yu T, Hubbard D, Ray A, Ghandehari H, In vivo biodistribution and pharmacokinetics of silica nanoparticles as a function of geometry, porosity and surface characteristics, Journal of controlled release, 163 (2012) 46–54. [PubMed: 22684119]

[15]. Herd H, Daum N, Jones AT, Huwer H, Ghandehari H, Lehr C-M, Nanoparticle geometry and surface orientation influence mode of cellular uptake, ACS nano, 7 (2013) 1961–1973. [PubMed: 23402533]

[16]. Cho M, Cho W-S, Choi M, Kim SJ, Han BS, Kim SH, Kim HO, Sheen YY, Jeong J, The impact of size on tissue distribution and elimination by single intravenous injection of silica nanoparticles, Toxicology letters, 189 (2009) 177–183. [PubMed: 19397964]

[17]. Kim Y-R, Lee S-Y, Lee EJ, Park SH, Seong N.-w., Seo H-S, Shin S-S, Kim S-J, Meang E-H, Park M-K, Toxicity of colloidal silica nanoparticles administered orally for 90 days in rats, International journal of nanomedicine, 9 (2014) 67.

[18]. Murugadoss S, Lison D, Godderis L, Van Den Brule S, Mast J, Brassinne F, Sebaihi N, Hoet PH, Toxicology of silica nanoparticles: an update, Archives of toxicology, 91 (2017) 2967–3010. [PubMed: 28573455]

[19]. Huang X, Li L, Liu T, Hao N, Liu H, Chen D, Tang F, The shape effect of mesoporous silica nanoparticles on biodistribution, clearance, and biocompatibility in vivo, ACS nano, 5 (2011) 5390–5399. [PubMed: 21634407]

[20]. Herd HL, Bartlett KT, Gustafson JA, McGill LD, Ghandehari H, Macrophage silica nanoparticle response is phenotypically dependent, Biomaterials, 53 (2015) 574–582. [PubMed: 25890753]

[21]. Herd HL, Malugin A, Ghandehari H, Silica nanoconstruct cellular toleration threshold in vitro, Journal of controlled release : official journal of the Controlled Release Society, 153 (2011) 40–48. [PubMed: 21342660]

[22]. Yazdimamaghani M, Moos PJ, Dobrovolskaia MA, Ghandehari H, Genotoxicity of amorphous silica nanoparticles:status and prospects, Nanomedicine: Nanotechnology, Biology and Medicine, (2018).

[23]. Lee S, Kim M-S, Lee D, Kwon TK, Khang D, Yun H-S, Kim S-H, The comparative immunotoxicity of mesoporous silica nanoparticles and colloidal silica nanoparticles in mice, International journal of nanomedicine, 8 (2013) 147. [PubMed: 23326190]

[24]. Yazdimamaghani M, Moos PJ, Ghandehari H, Global gene expression analysis of macrophage response induced by nonporous and porous silica nanoparticles, Nanomedicine : nanotechnology, biology, and medicine, 14 (2018) 533–545.

[25]. Borm PJ, Fowler P, Kirkland D, An updated review of the genotoxicity of respirable crystalline silica, Particle and fibre toxicology, 15 (2018) 23. [PubMed: 29783987]

[26]. Saikia J, Mohammadpour R, Yazdimamaghani M, Northrup H, Hlady V, Ghandehari H, Silica nanoparticle–endothelial interaction: Uptake and Effect on Platelet Adhesion under Flow Conditions, ACS Applied Bio Materials, 1 (2018) 1620–1627.

[27]. Saikia J, Yazdimamaghani M, Hadipour Moghaddam SP, Ghandehari H, Differential protein adsorption and cellular uptake of silica nanoparticles based on size and porosity, ACS applied materials & interfaces, 8 (2016) 34820–34832. [PubMed: 27998138]

[28]. Mohammadpour R, Yazdimamaghani M, Reilly C, Ghandehari H, Transient Receptor Potential (TRP) Ion channel-dependent toxicity of silica nanoparticles and Poly (amido amine)(PAMAM) dendrimers, The Journal of pharmacology and experimental therapeutics, (2018).

[29]. Hadipour Moghaddam SP, Saikia J, Yazdimamaghani M, Ghandehari H, Redox-responsive polysulfide-based biodegradable organosilica nanoparticles for delivery of bioactive agents, ACS applied materials & interfaces, 9 (2017) 21133–21146. [PubMed: 28609092]

[30]. Huber SA, Pfaeffle B, Differential Th1 and Th2 cell responses in male and female BALB/c mice infected with coxsackievirus group B type 3, Journal of Virology, 68 (1994) 5126–5132. [PubMed: 8035512]

[31]. Weinstein Y, Ran S, Segal S, Sex-associated differences in the regulation of immune responses controlled by the MHC of the mouse, The Journal of Immunology, 132 (1984) 656–661. [PubMed: 6228595]

[32]. Krzych U, Thurman GB, Goldstein AL, Bressler JP, Strausser HR, Sex-Related Immunocompetence of BALB/c Mice: I. Study of Immunologic Responsiveness of Neonatal, Qeanling, and Young Adult Mice, The Journal of Immunology, 123 (1979) 2568–2574. [PubMed: 159320]

[33]. Ivanov S, Zhuravsky S, Yukina G, Tomson V, Korolev D, Galagudza M, In vivo toxicity of intravenously administered silica and silicon nanoparticles, Materials, 5 (2012) 1873–1889.

[34]. He Q, Zhang Z, Gao F, Li Y, Shi J, In vivo biodistribution and urinary excretion of mesoporous silica nanoparticles: effects of particle size and PEGylation, small, 7 (2011) 271–280. [PubMed: 21213393]

[35]. Kumar R, Roy I, Ohulchanskky TY, Vathy LA, Bergey EJ, Sajjad M, Prasad PN, In vivo biodistribution and clearance studies using multimodal organically modified silica nanoparticles, ACS nano, 4 (2010) 699–708. [PubMed: 20088598]

[36]. Nishimori H, Kondoh M, Isoda K, Tsunoda S.-i., Tsutsumi Y, Yagi K, Histological analysis of 70-nm silica particles-induced chronic toxicity in mice, European Journal of Pharmaceutics and Biopharmaceutics, 72 (2009) 626–629. [PubMed: 19341796]

[37]. Lokwani DP, The ABC of CBC : interpretation of complete blood count and histograms, First edition ed., Jaypee Brothers Medical Publishers (P) Ltd, New Delhi, 2013.

[38]. Yu T, Malugin A, Ghandehari H, Impact of silica nanoparticle design on cellular toxicity and hemolytic activity, ACS nano, 5 (2011) 5717–5728. [PubMed: 21630682]

[39]. Schutz I, Lopez-Hernandez T, Gao Q, Puchkov D, Jabs S, Nordmeyer D, Schmudde M, Ruhl E, Graf CM, Haucke V, Lysosomal dysfunction caused by cellular accumulation of silica nanoparticles, The Journal of biological chemistry, 291 (2016) 14170–14184. [PubMed: 27226546]

[40]. Yu Y, Li Y, Wang W, Jin M, Du Z, Li Y, Duan J, Yu Y, Sun Z, Acute toxicity of amorphous silica nanoparticles in intravenously exposed ICR mice, PloS one, 8 (2013) e61346. [PubMed: 23593469]

[41]. Waegeneers N, Brasseur A, Van Doren E, Van der Heyden S, Serreyn P-J, Pussemier L, Mast J, Schneider Y-J, Ruttens A, Roels S, Short-term Biodistribution and clearance of intravenously administered silica nanoparticles, Toxicology Reports, (2018).

[42]. Zhuravskii S, Yukina G, Kulikova O, Panevin A, Tomson V, Korolev D, Galagudza M, Mast cell accumulation precedes tissue fibrosis induced by intravenously administered amorphous silica nanoparticles, Toxicology mechanisms and methods, 26 (2016) 260–269. [PubMed: 27055490]

[43]. Xie G, Sun J, Zhong G, Shi L, Zhang D, Biodistribution and toxicity of intravenously administered silica nanoparticles in mice, Archives of toxicology, 84 (2010) 183–190. [PubMed: 19936708]

[44]. Herd HL, Malugin A, Ghandehari H, Silica nanoconstruct cellular toleration threshold in vitro, Journal of controlled release, 153 (2011) 40–48. [PubMed: 21342660]

[45]. Feghali CA, Wright TM, Cytokines in acute and chronic inflammation, Front Biosci, 2 (1997) d12–d26. [PubMed: 9159205]

[46]. Turner MD, Nedjai B, Hurst T, Pennington DJ, Cytokines and chemokines: At the crossroads of cell signalling and inflammatory disease, Biochimica et biophysica acta, 1843 (2014) 2563–2582. [PubMed: 24892271]

[47]. Arango Duque G, Descoteaux A, Macrophage cytokines: involvement in immunity and infectious diseases, Frontiers in immunology, 5 (2014) 491. [PubMed: 25339958]

[48]. Kleemann R, Zadelaar S, Kooistra T, Cytokines and atherosclerosis: a comprehensive review of studies in mice, Cardiovascular research, 79 (2008) 360–376. [PubMed: 18487233]

[49]. Zamboni WC, Szebeni J, Kozlov SV, Lucas AT, Piscitelli JA, Dobrovolskaia MA, Animal models for analysis of immunological responses to nanomaterials: Challenges and considerations, Advanced drug delivery reviews, 136-137 (2018) 82–96. [PubMed: 30273617]

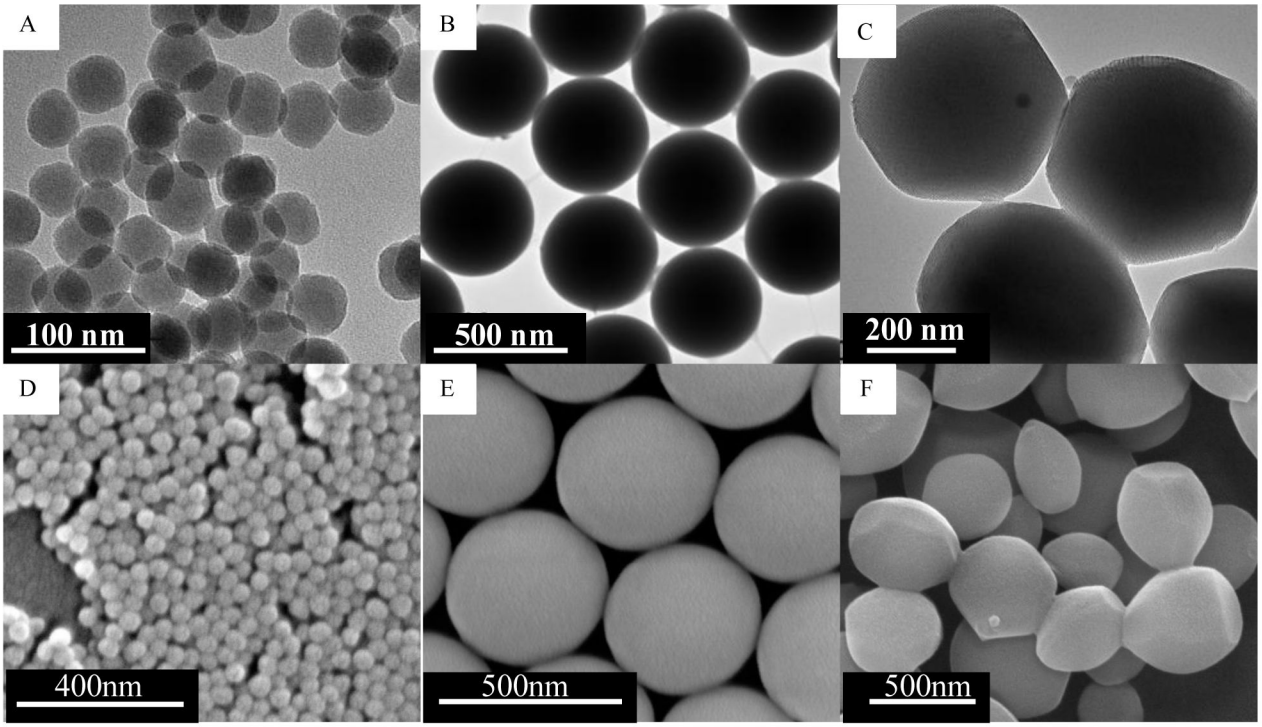

Figure 1.

Transmission electron microscopy images of (A) Stöber SNPs50 with average diameter of 46 ± 4.9 nm, (B) Stöber SNPs500 with average diameter of 432 ± 18.7 nm, (C) mesoporous SNPs500 with average diameter of 466 ± 86 nm. Scanning electron microscopy images of (D) Stöber SNPs50, (E) Stöber SNPs500, (F) MSNPs500.

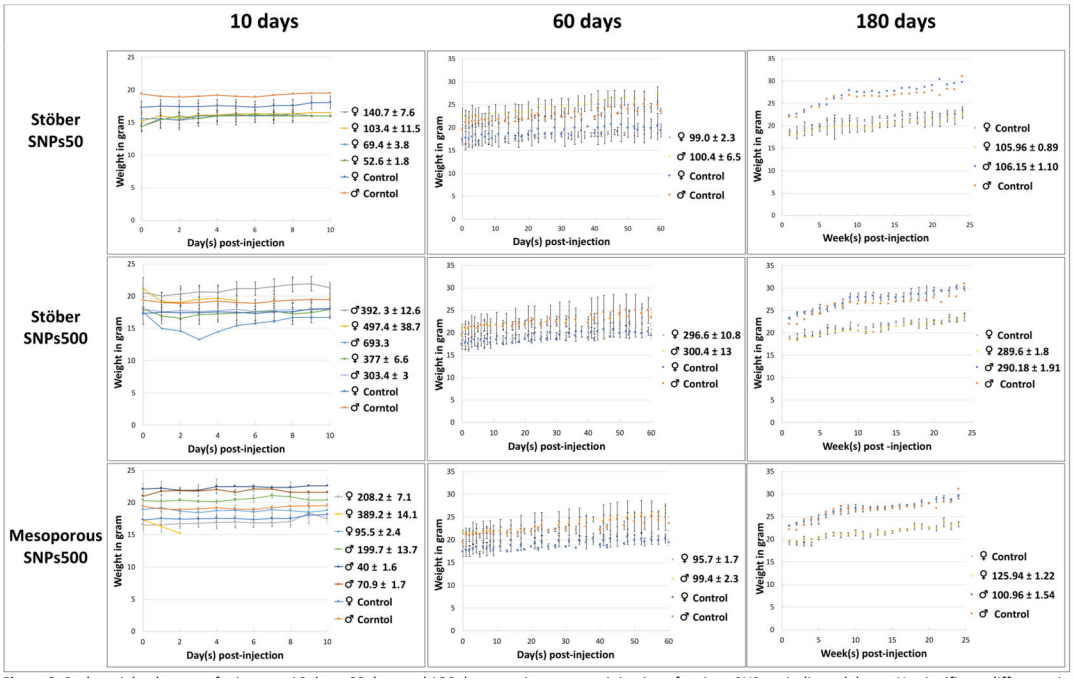

Figure 2.

Body weight changes of mice over 10 days, 60 days and 180 days post intravenous injection of various SNPs at indicated doses. No significant difference in weight gain was observed between treatment groups and they had the same trend as control group for each injection phase except mice who received Stöber SNPs500 10 days after injection as described in Table 2. Values in the Figure are shown in mg.kg^{-1}.

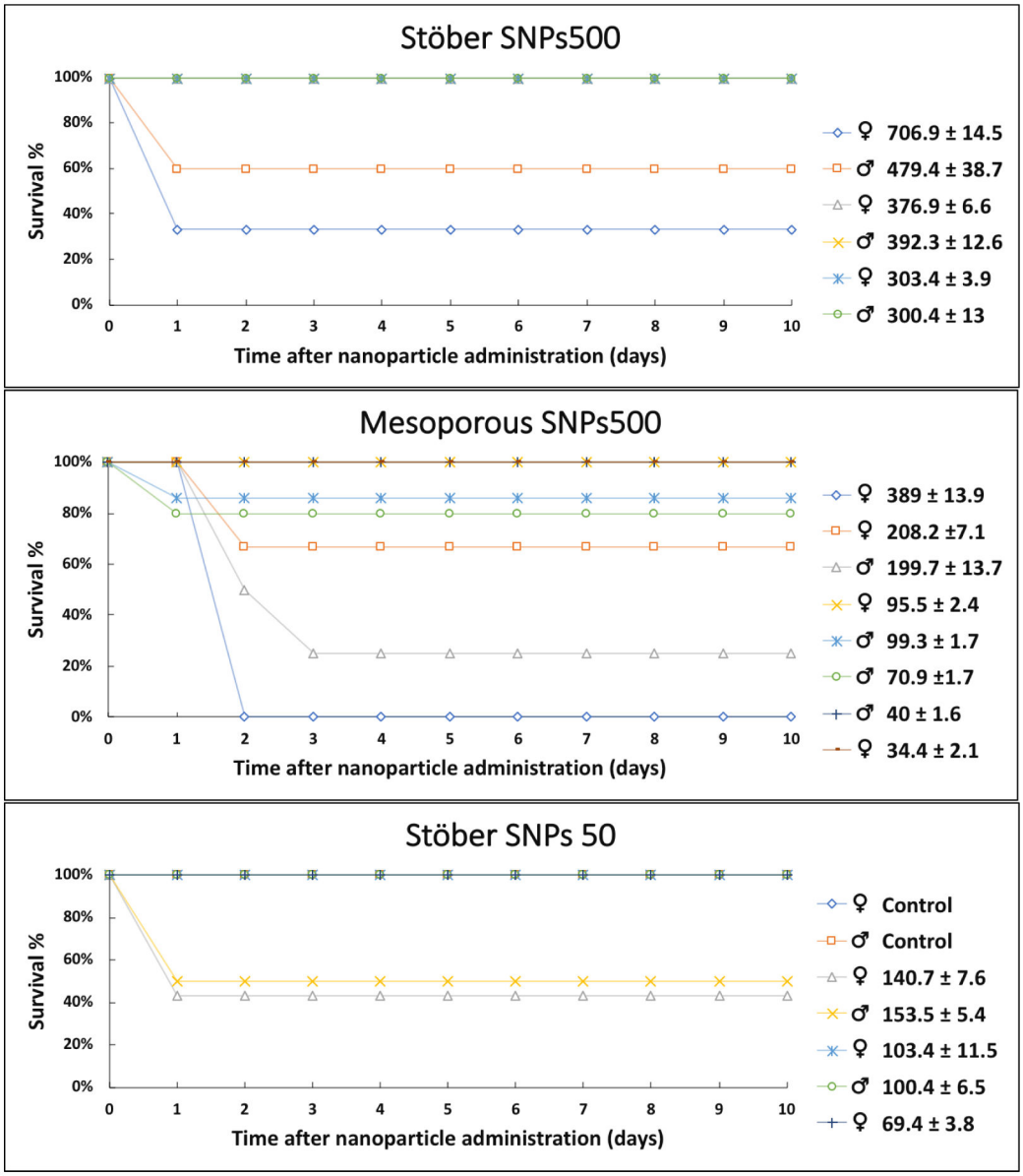

Figure 3.

Survival graphs of BALB/c mice 10 days post injection with different SNPs. Values in the Figure are shown as $mg.kg^{-1}$.

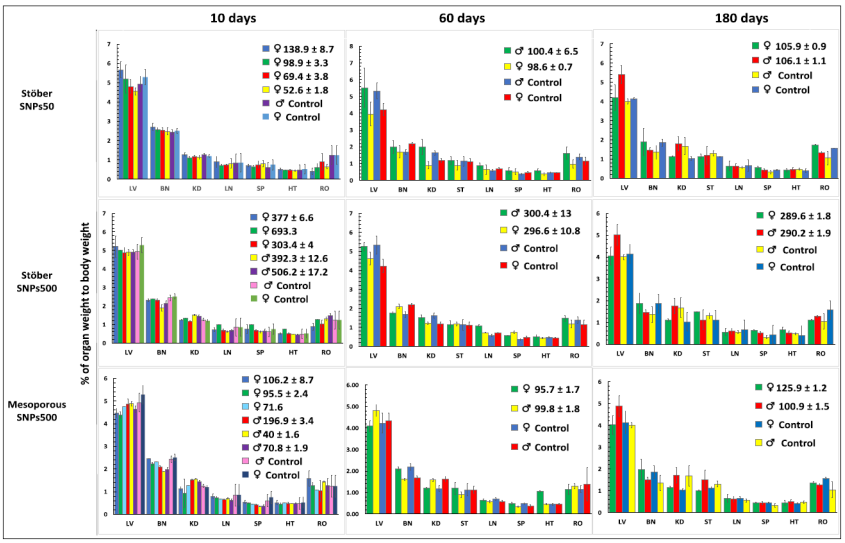

Figure 4.

Normalized organ to body weight ratio for mice that were administrated with different SNPs at indicated doses and survived for 10 days, 60 days and 180 days. There was no significant difference in organ weight percentages between treatment groups and control groups. Doses are shown in the Figure as $mg.kg^{-1}$. Abbreviations: liver (LV), brain (BN), kidney (KD), lung (LN), spleen (SP), heart (HT) and reproductive organs (RO).

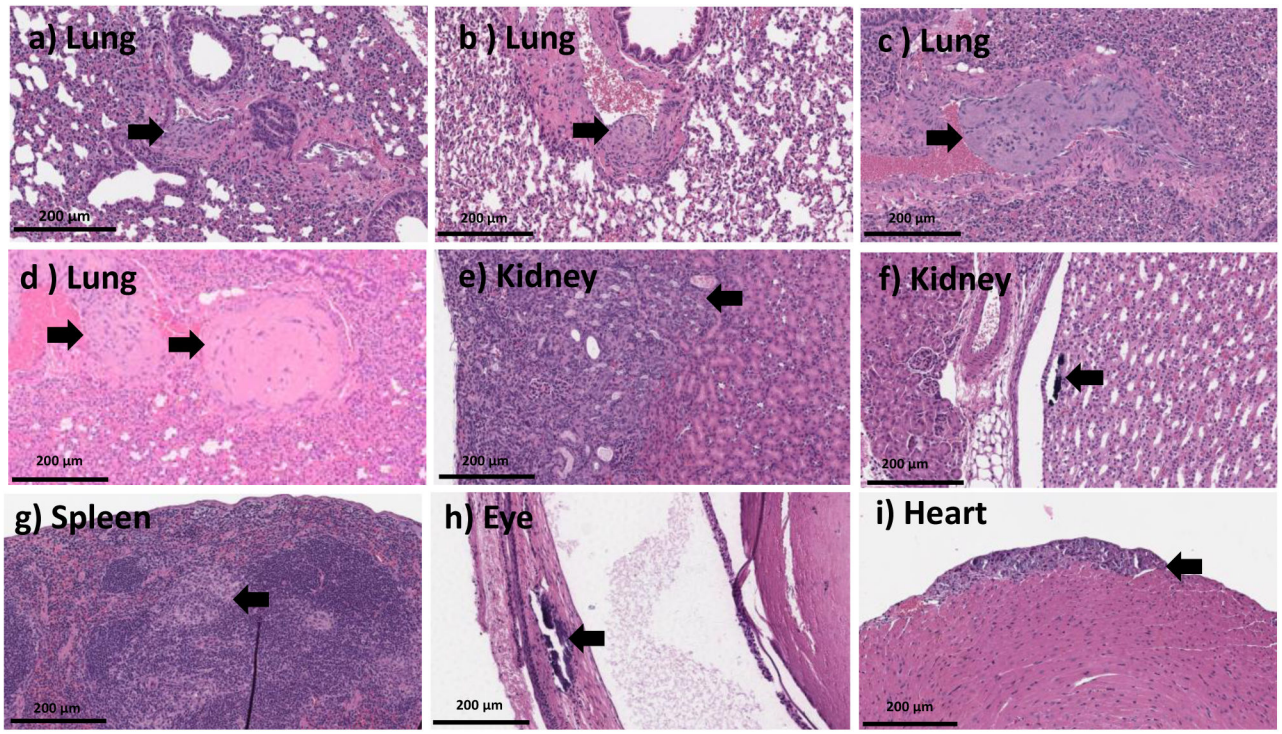

Figure 5.

20X H and E microscopic images from the organs of the mice which recovered from MSNPs500 (at dose range of ~200-389 mg.kg^{-1}) (a-f, h-i) and Stöber SNPs50(at dose range of ~241-153 mg.kg^{-1}) (g) 10 days post injection. This data shows lung tissue with organizing thrombosis involving larger pulmonary vessels (a-d), wedge shaped injury of the renal parenchyma, in keeping with infarction (e), focal calcifications inside the renal pelvis (f), spleen with aggregates of foamy histocytes (g), focal retinal calcifications (h), and focal calcified myocytes (i). Histologic abnormalities are marked with the black arrow.

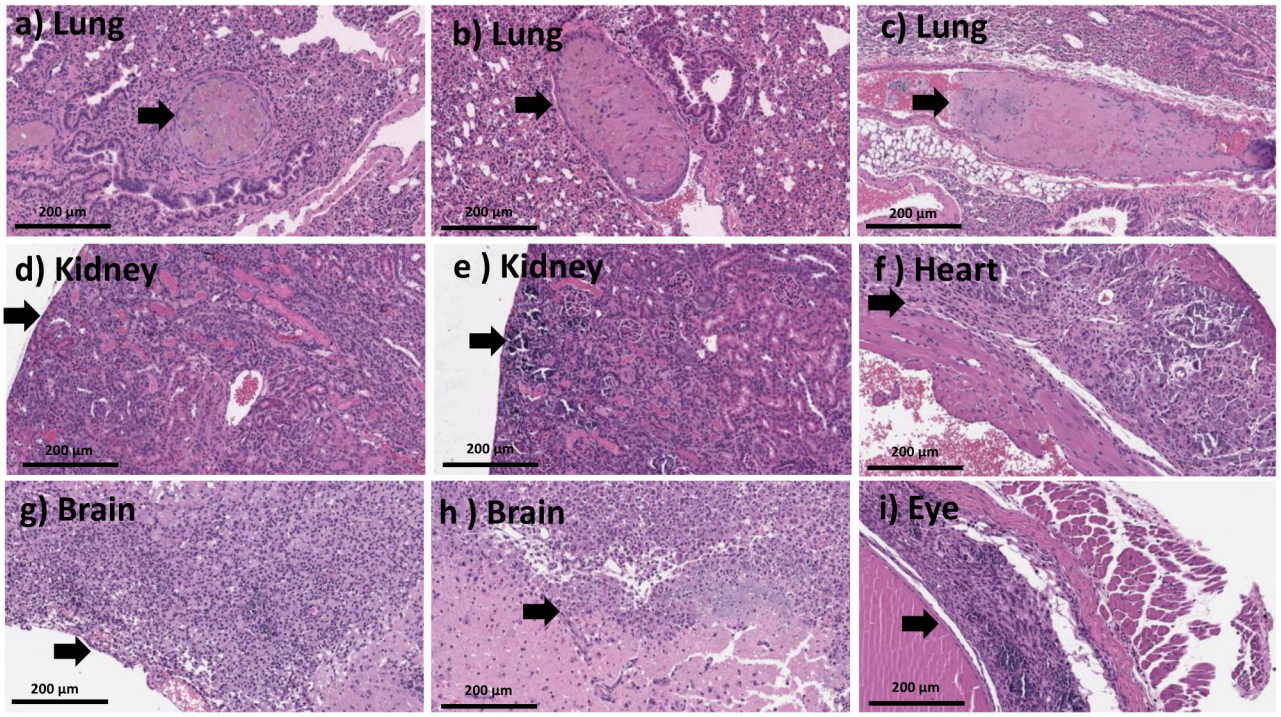

Figure 6.

20X H and E images from mice treated with high dose (>MTD (~392-707 mg.kg^{-1})) of Stöber SNPs500 for 10 days depicting organizing thrombi within pulmonary vessels (a-c), focal renal parenchymal damage, which appeared consistent with infarction (d-e), fibrosis and calcifications within cardiac wall, in keeping with older infarction (f), organizing brain infarcts with necro inflammatory infiltrate (g-h), marked retinal injury with calcification and gliosis (i). Black arrows point towards the histologic abnormalities.

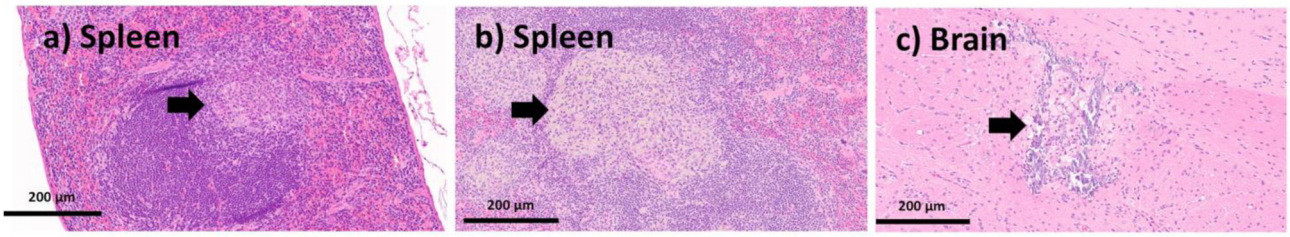

Figure 7.

20X H and E images from mice treated with Stöber SNPs50 at 60 days (a) and Stöber SNPs500 at 60 days (b-c), showing aggregates of foamy histocytes with admixed neutrophils within the splenic tissue (black arrow, a and b) and focal injury of the brain tissue with necrosis, macrophages and calcifications, likely representing a small infarction (black arrow, c).

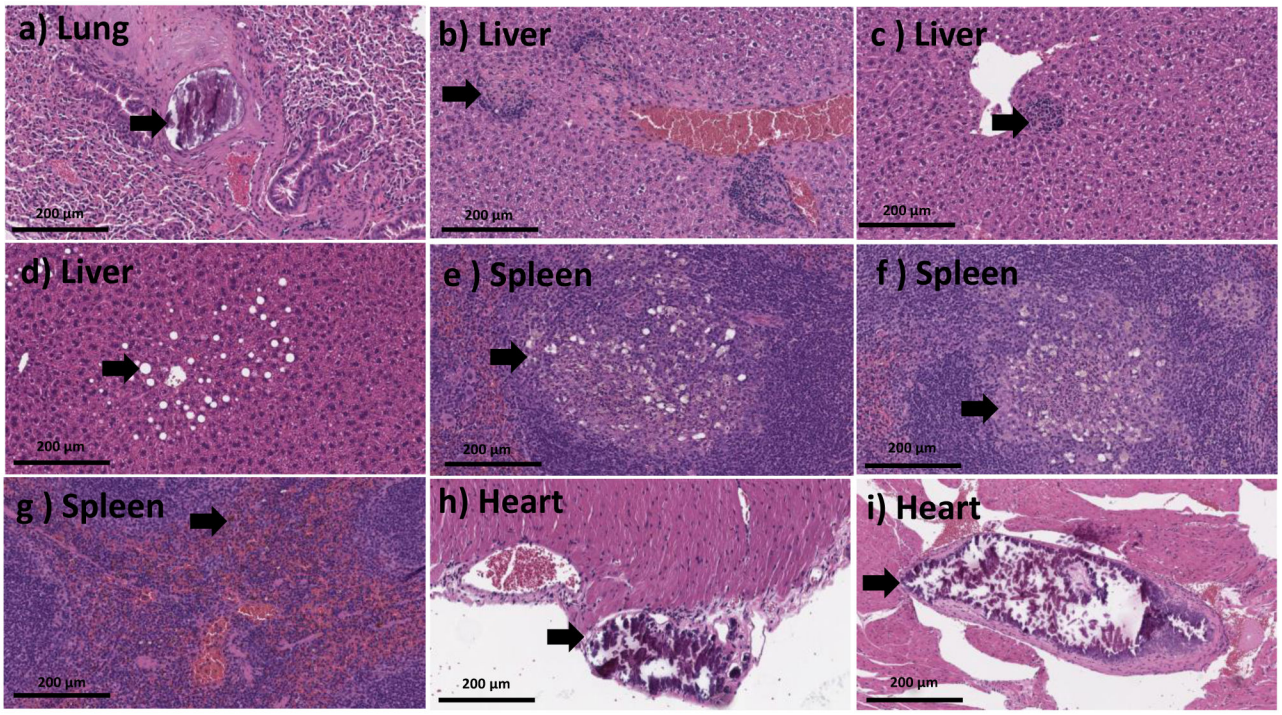

Figure 8.

20X H and E images from mice treated with large Stöber SNPs500 and MSNPs500 for mice that survived for 180 days. Panels show thrombosis with calcification within the pulmonary vasculature (a), small aggregates of mostly lobular inflammation composed of admixed lymphocytes and ceroid laden macrophages within the liver tissue (b-c), mild macrovesicular steatosis within approximately 5% of zone 3 hepatocytes (d), aggregates of foamy histocytes with admixed neutrophils found in the spleen (e-f), focal hemosiderin deposition in the splenic tissue (g), small focus of calcified myocytes (h) and organizing thrombosis with calcification within the ventricle of the heart (i).

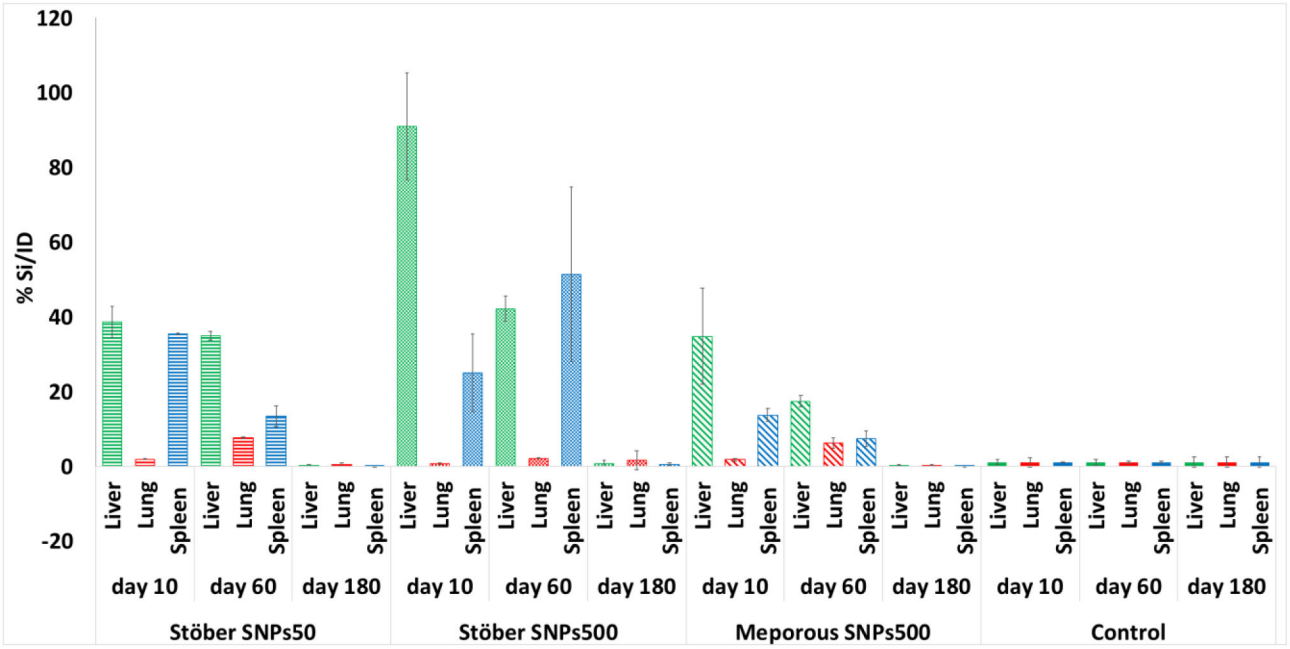

Figure 9.

Silicon accumulation measurement over time in liver, lung and spleen of injected mice (MTD). Although liver and spleen accumulate the most silicon after 10 days and 60 days, the silicon content in all mice after 180 days was negligible which means the particles were cleared from these tissues.

Gene Expression Analysis of Inflammation Pathways after Acute and Subchronic Exposure to SNPs

NPs:	SNPs50									MSNPs500									SNPs500								
Organ:	Liver			Spleen			Lung			Liver			Spleen			Lung			Liver			Spleen			Lung		
Day:	D10	D60	D180	D10	D60	D180	D10	D60	D180	D10	D60	D180	D10	D60	D180	D10	D60	D180	D10	D60	D180	D10	D60	D180	D10	D60	D180
Csf2	-13.7	-1.8	2.0	-4.6	-4.9	-8.5	-4.1	1.7	1.5	18.3	72.3	5.7	-1.6	11.4	-11.9	-21.3	-2.9	-1.4	13.7	15.7	40.3	-2.3	4.0	-7.5	-54.8	-1.4	1.1
Cxcr2	-3.1	6.1	2.4	-1.3	-5.4	1.1	19.0	1.3	1.2	-27.8	24.0	1.8	2.5	-2.1	-1.2	-1.2	1.3	5.8	5.5	14.3	-1.4	-2.4	-7.9	3.2	1.4	1.5	8.7
IL1β	-3.9	6.5	1.4	-1.4	-7.2	-2.7	-1.2	-4.0	1.1	28.3	4.0	2.0	2.8	-2.2	-4.7	5.4	-3.8	-2.0	6.0	3.9	1.4	1.4	1.3	-5.1	-1.5	-5.6	-1.2
IL6	-29.0	10.2	2.0	-3.4	-2.0	-4.1	14.4	-4.0	1.4	-4.5	77.5	-1.4	-1.5	-1.2	-6.9	1.5	1.4	1.8	1.7	32.0	2.4	-4.1	-1.1	-10.3	5.1	-3.3	4.3
TNFα	-1.3	9.3	4.2	-1.1	-1.4	-5.2	-1.6	-1.5	2.9	1.9	20.3	2.3	1.2	-1.7	-7.0	-1.8	4.1	1.4	7.4	10.0	6.1	-2.3	-1.3	-8.2	-4.5	1.1	2.4
IL10	-8.6	2.4	2.2	-2.0	-1.3	-11.2	-20.3	-1.3	2.7	-1.3	96.5	1.9	-2.5	-1.3	-62.4	-5.7	7.8	-1.5	1.0	28.5	5.8	-2.1	2.1	-43.9	-11.5	-1.1	-1.1
IL12	-4.2	18.8	-1.5	-1.3	-2.2	-4.1	-5.4	1.3	-2.2	-1.1	58.4	-1.7	1.7	-3.8	-12.8	-6.7	4.5	-9.1	-0.3	45.0	4.2	-0.6	2.1	-18.2	-3.2	-1.2	-4.5
IL4	-8.2	2.7	-1.3	1.3	-3.5	-4.4	-1.2	1.1	1.3	1.5	23.3	-1.0	2.5	-2.7	-17.9	-1.7	2.2	-1.2	4.5	8.5	1.6	1.9	-3.1	-25.7	-1.6	-1.5	2.2
IL5	-18.5	7.2	2.4	-10.7	1.4	-14.8	4.5	-1.3	-1.0	-2.3	238.1	8.5	-4.0	4.1	-7.7	-2.6	-2.5	1.8	2.6	98.0	17.9	-12.5	-1.8	-9.6	-2.3	-2.3	2.0
INFγ	-36.2	5.4	3.4	-2.1	-3.1	-1.6	-6.5	-2.4	4.4	-1.9	68.9	2.6	1.3	-1.9	-2.6	-3.1	4.1	-1.6	1.2	38.5	1.1	-1.3	1.2	-6.2	-3.8	-1.0	1.2

Figure 10.

Heat map profile of inflammatory cytokine gene expressions in tissues of the mice that received Stöber SNPs50, Stöber SNPs500 and mesoporous SNPs, MSNPs500 at the MTD on day 10, 60 and 180 post intravenous administration. The values are the relative gene expression to saline treated mice which normalized to GAPDH mRNA levels as reference gene using ΔΔCT method. Gradient blue and red color shows downregulation and upregulation of the indicated genes, respectively.

Table 1:

A) Mortality and morbidity of Balb/c mice post intravenous injection of various doses of SNPs. B) MTD of SNPs of male and female Balb/c mice 10 days post-administration.

Mortality and Morbidity				
Treatment	**Sex**	**Dose (mg/kg)**	**Mortality**	**Morbidity**
Control	♀	N/A	0/5	0
	♂	N/A	0/5	0
Stöber SNPs50	♀	141 ± 8	4/7	0/3
	♂	153 ± 5	2/4	0/2
	♀	103 ± 11	0/6	0/6
	♂	100 ± 6	0/6	0/6
	♀	69 ± 4	0/5	0/5
MSNPs500	♀	389 ± 14	3/3	N/A
	♀	208 ± 7	1/3	0/2
	♂	200 ± 13	2/4	0/2
	♀	95 ± 2	0/5	0/5
	♂	99 ± 2	1/5	0/5
	♂	71 ± 2	1/5	0/4
	♂	40 ± 2	0/5	0/5
Stöber SNPs500	♀	707 ± 14	2/3	1/1
	♂	479 ± 39	2/5	1/3
	♀	377 ± 6	0/3	3/3
	♂	392 ± 12	0/5	3/5
	♀	303 ± 4	0/5	0/5
	♂	300 ± 13	0/5	0/5

(A)

Maximum Tolerated Dose (MTD)			
	Stöber SNPs50	MSNPs500	Stöber SNPs500
♀ Balb/c Mice	103 ± 11 mg.kg^{-1} ¥	95 ± 2 mg.kg^{-1}	303 ± 4 mg.kg^{-1}
♂ Balb/c Mice	100 ± 6 mg.kg^{-1}	40 ± 2 mg.kg^{-1}	300 ± 13 mg.kg^{-1}

€ Absence of morbidity, mortality, or > 10% weight loss 10 days after iv injection (n=5/NP/sex).

(B)

Table 2.

Clinical observation of the mice injected with SNPs at indicated doses. Time of death, significant decrease in animal weight and signs of morbidity for the mice mentioned in Table 1 are described here.

Clinical Observation							
Time	**Nanoparticles**	**Female**			**Male**		
		Time of Death	**Weight Loss**	**Morbidity**	**Time of Death**	**Weight Loss**	**Morbidity**
10 days	Stöber SNPs50 (ID > MTD)	5-24 hr post-injection	NO	NO	6-24 hr post-injection	Up to 11%	NO
	Mesoporous SNPs500 (ID > MTD)	2-3 days post-injection	Up to 10%	Signs of moderate pain for example: hunched posture, rough hair, slow movements	1-3 days post-injection	Up to 6%	Signs of moderate pain for example: shivering, sunken eye, rough hair.
	Stöber SNPs500 (ID > MTD)	24 hr post-injection	Up to 24%	Signs of severe pain for example: shivering, rough hair, slow movements, weakness, blindness, hemiplegia, paralysis, necrosis at the end of tail, violent reaction to stimuli or when approached, non-responsive when coaxed, ataxia and pacing around in circles, changes in respiration	24 hr post-injection	Up to 16.14%	Signs of severe pain for example: shivering, sensitive to handling, back leg weakness and rigidity, very rough hair, squinted and sunken eye, violent reactions or non-responsive to stimuli or when approached, non-responsive when coaxed, ataxia and circling, changes in respiration, hemiplegia
	Stöber SNPs50 (MTD)	No significant clinical abnormalities were observed.			No significant clinical abnormalities were observed.		
	Mesoporous SNPs500 (MTD)						
	Stöber SNPs500 (MTD)						
60 days	Stöber SNPs50 (MTD)	No significant clinical abnormalities were observed.			No significant clinical abnormalities were observed.		
	Mesoporous SNPs500 (MTD)						
	Stöber SNPs500 (MTD)						
180 days	Stöber SNPs50 (MTD)	No significant clinical abnormalities were observed.			No significant clinical abnormalities were observed.		
	Mesoporous SNPs500 (MTD)						
	Stöber SNPs500 (MTD)						

Table 3.

Hematological profile of the mice treated with SNPs. The values are presented as red, blue and yellow colors which mean high, low and normal ranges, respectively. The gradient in high and low dose represented the percentage of the animals (e.g., dark red means 70-100% animals in those groups showed high level of the studied parameters). Abbreviations: Neutrophil (NEU), Lymphocyte (LYM), Monocyte (MONO), Eosinophil (EOS), Basophil (BAS), Red Blood Cell (RBC), Hemoglobin (HGB), Hematocrit (HCT), Mean Corpuscular Hemoglobin (MCH), Mean Corpuscular Hemoglobin Concentration (MCHC), Red Blood Cell Distribution Width (RDW), Platelet (PLT) and Mean Platelet Volume (MPV) level.

Blood Cell Count Annalysis																
Time	**Treatment**	**Sex**	**Concentration (mg/kg)**	**NEU**	**LYM**	**MONO**	**EOS %**	**BAS %**	**RBC**	**HGB**	**HCT %**	**MCH**	**MCHC**	**RDW %**	**PLT**	**MPV**
10 days	**Stöber SNPs50**	♀	>MTD													
			MTD													
			<MTD													
			<<MTD													
	Stöber SNPs500	♀	>>MTD													
			>MTD													
			MTD													
		♂	>MTD													
			>>MTD													
	Mesoporous SNPs500	♀	MTD													
			<MTD													
			<<MTD													
		♂	<<MTD													
			<MTD													
			MTD													
	Control	♀	Control													
		♂	Control													
60 days	**Stöber SNPs50**	♀	MTD													
		♂	MTD													
	Stöber SNPs50	♀	MTD													
		♂	MTD													

Blood Cell Count Annalysis															
Time	**Treatment**	**Sex**	**Concentration (mg/kg)**	**NEU**	**LYM**	**MONO**	**EOS %**	**BAS %**	**RBC**	**HGB**	**HCT %**	**MCH**	**MCHC**	**RDW %**	**PLT**	**MPV**
	Mesoporous SNPs500	♀	MTD													
		♂	MTD													
	Control	♀	Control													
		♂	Control													
180 days	**Stöber SNPs50**	♀	MTD													
		♂	MTD													
	Stöber SNPs500	♀	MTD													
		♂	MTD													
	Mesoporous SNPs500	♀	MTD													
		♂	MTD													
	Control	♀	Control													
		♂	Control													
			Table Guidline:	high						low						Normal
				70-100%		50-70%		30-50%		70-100%		50-70%		30-50%		

Table 4.

Plasma biochemistry values for the mice administrated SNPs, intravenously at indicated doses. The results show significant changes in plasma parameters of BALB/c female and male mice after SNP intravenous administration. Abbreviations: blood urea nitrogen (BUN), alanine aminotransferase (ALT), aspartate aminotransferase (AST), alkaline phosphatase (ALP).

Animal Treatment Groups		Serum Parameter				
		BUN (mg/dl)	Glucose (mg/dl)	ALT (U/L)	AST (U/L)	ALP (U/L)
	Normal Range	20-26	190-280	10-190	10-380	0-260
10 days	♀Control	17.2 ± 1.1	146 ± 14.3	34 ± 10.2	239.5 ± 56.5	241 ± 41.1
	♂ Control	17.2 ± 2.1	142 ± 13.3	168 ± 17.7	120.5 ± 22.2	124.7 ± 16.6
	Stöber SNPs50 (♀65.51 ±2.8 mg.kg^{-1})	18.6 ± 3.2	168 ± 18.8	22 ± 6.7	124.7 ± 18.4	120.5 ± 11.1
	Stöber SNPs500 (♂392 ± 14.61 mg.kg^{-1}.	19.8 ± 0.8	148 ± 22.2	52.2 ± 12.2	296.7 ± 49.8	218.3 ± 53.2
	Stöber SNPs500 (♂506 ± 17.02 mg.kg^{-1})	18.8 ± 2	170.3 ± 18.1	47.5 ± 0.7	191.3 ± 37.2	160 ± 30.5
	Stöber SNPs500 (♀374.56 ± 7.29 mg.kg^{-1})	22.3 ± 4.5	164.5 ± 21.9	106 ±19.4	335 ±54.2	192 ± 23.4
	Stöber SNPs500 (♀303.36 ± 3.99 mg.kg^{-1})	15.9 ± 0.9	193 ± 27.9	68 ± 17.6	238.7 ± 39.5	169.5 ± 43.5
	Mesoporous SNPs500 (♂196.91 ± 3.38 mg.kg^{-1})	19.9 ± 5	165 ± 22.6	56 ± 22.6	260.5 ± 12.4	221.5 ± 88.3
	Mesoporous SNP500 (♂40.05 ± 1.62 mg.kg^{-1})	17.3 ± 1	187.4 ± 27	34.2 ± 8.8	147.4 ± 59.1	127.6 ± 37.5
	Mesoporous SNPs500 (♂70.8 ± 1.96 mg.kg^{-1})	22.3 ± 3.3	182 ± 21.5	43.7 ± 9	202.2 ± 34.2	199.3 ± 48.6
	Mesoporous SNPs500 (♀206.15 ± 8.74 mg.kg^{-1})	13.4 ± 0.3	244 ± 39.6	24 ± 1.4	94 ± 1.4	120.5 ± 16.2
	Mesoporous SNPs500 (♀96.73 ± 1.1 mg.kg^{-1})	16.6 ±0.07	158.5 ± 30.4	48 ± 4.2	304.5 ± 68.5	231 ± 43.8
60 days	♀Control	23.7 ± 1.5	237.5 ± 11.9	28.7 ± 4.9	99 ± 22	63.2 ± 4.1
	♂ Control	22.2 ± 4	220.5 ± 16.4	28.7 ± 3.5	81.5 ± 20.5	56.2 ± 9
	Stöber SNPs50 (♀98.81 ± 0.68 mg.kg^{-1})	21.2 ± 0.7	190.6 ± 25.1	37.3 ± 7.7	166 ± 51.6	87 ± 9.5
	Stöber SNPs50 (♂100.44 ± 6.49 mg.kg^{-1})	18.6 ± 2.8	181.3 ± 18.3	47.3 ± 19.8	164.2 ± 42	110.3 ± 43.5
	Stöber SNPs500nm (♀ 295 ± 6.82 mg.kg^{-1})	19.7 ± 2.7	194.3 ± 12.9	35 ± 7	108.5 ± 34.9	61.6 ± 3.2
	Stöber SNPs500 (♂298.06 ± 8.91 mg.kg^{-1})	27.7 ± 5.9	210.2 ± 19.9	34 ± 5	102 ± 30.9	58.8 ± 9.3
	Mesoporous SNPs500 (♀96.08 ± 0.59 mg.kg^{-1})	26.5 ± 8	226.6 ± 14.3	22 ± 1.7	64.3 ± 13	64 ± 4.5
	Mesoporous SNP500 (♂99.69 ± 2.72 mg/kg^{-1})	19.2 ± 2.3	224.2 ±18.5	35 ± 1.7	105.8 ± 19.8	52.6 ± 8.5
180 days	♀Control	18.4 ± 7	139.5 ± 14.1	22.5 ± 2.1	74.5 ± 2.1	49 ± 4.2
	♂ Control	25.2 ± 6.1	142 ± 17.3	25 ± 3.7	58 ± 7.5	41 ± 6.6
	Mesoporous SNPs500 (♀97.4 ± 3.7 mg.kg^{-1})	18.6 ± 2.9	137.5 ± 17.6	23.5 ± 4.9	77.6 ± 12.4	51 ± 9.8
	Stöber SNPs500 (♀290.16 ± 2.21 mg.kg^{-1})	20.3 ± 2.2	187.5 ± 60.1	24 ± 5.6	75.5 ± 7.7	47.5 ± 2.1
	Stöber SNPs50 (♀103.12 ± 2.77 mg.kg^{-1})	22.2 ± 5.1	133.5 ± 6.3	24 ± 1.7	79 ± 18.2	58.5 ± 3.5
	Mesoporous SNPs500 (♂101.69 ± 1.26 mg.kg^{-1})	25.1 ± 2.3	100 ± 11.3	28.5 ± 9.1	70.5 ± 14.8	39.5 ± 4.9
	Stöber SNPs500 (♂291.15 ± 1.77 mg.kg^{-1})	24.3 ± 3.7	106.5 ± 9.2	26.5 ± 2.2	75 ± 11.3	38.5 ± 4.9
	Stöber SNPs50 (♂106.15 ± 1.35 mg.kg^{-1})	28.5 ± 9.3	75 ± 4.3	25 ± 1.4	81 ± 15.5	41 ± 5.7

Table 5:

Summary of tissue toxicity of silica nanoparticles as a function of size, porosity and time. ** and * mean all the mice (3 out of 3) or 1 or 2 out of 3 mice, respectively, showed abnormal lesions in related tissue, “x” means the tissue of all the mice that received the indicated nanoparticles looked healthy.

Affected organs based on histology results									
Nanoparticles	**10 days**			**60 days**			**180 days**		
	Liver	**Lung**	**Spleen**	**Liver**	**Lung**	**Spleen**	**Liver**	**Lung**	**Spleen**
Stöber SNPs500 (♀: 303 ± 4 mg.kg^{-1}) (♂: 300 ± 13 mg.kg^{-1})	**	**	**	**	*	*	*	x	X
Mesoporous SNPs500 (♀: 95 ± 2 mg.kg^{-1}) (♂: 40 ± 2 mg.kg^{-1})	**	**	**	*	x	x	*	x	x
Stöber SNPs50 (♀: 103 ± 11 mg.kg^{-1}) (♂: 100 ± 6 mg.kg^{-1})	**	x	x	x	x	**	x	x	X